Inorganic Chemistry

Article

pubs.acs.org/IC

Reactivity of the Anionic Diphosphorus Complex $[Mo_2Cp_2(\mu\text{-}PCy_2)(\mu\text{-}\kappa^2\text{:}\kappa^2\text{-}P_2)(CO)_2]^-$ toward Phosphorus- and Transition Metal-Based Electrophiles

M. Angeles Alvarez,[†] M. Esther García,[†] Daniel García-Vivó,[†] Raquel Lozano,[†] Alberto Ramos,*[,‡] and Miguel A. Ruiz*[,†]

[†]Departamento de Química Orgánica e Inorgánica/IUQOEM, Universidad de Oviedo, E-33071 Oviedo, Spain

[‡]Instituto Nacional del Carbón, CSIC, Francisco Pintado Fe 26, E-33011 Oviedo, Spain

Supporting Information

ABSTRACT: The reactions of the Li^+ salt of the title anion with chlorophosphines PR_2Cl (R = Cy, Ph, ^{t}Bu) led in all cases to products of formula $[Mo_2Cp_2(\mu\text{-}PCy_2)(\mu\text{-}\kappa^2_{P,P'}\text{:}\kappa^2_{P,P''}\text{-}P_2PR_2)(CO)_2]$, with the PR_2 group inserted in one of the Mo−P(basal) bonds of the anion to give novel tridentate phosphinodiphosphenyl ligands, as confirmed by the solid-state structure of the PCy_2 compound. When R was the bulky ^{t}Bu group, this product was in equilibrium with an isomer of formula $[Mo_2Cp_2(\mu\text{-}PCy_2)(\mu\text{-}\kappa^2_{P,P'}\text{:}\kappa^2_{P,P'}\text{-}P_2P^tBu_2)(CO)_2]$, in which the diphosphorus ligand of the anion binds the P^tBu_2 group through the lone pair of electrons at the basal P atom in an "end-on" fashion (computed P−P−P^tBu_2 = 114.7°); the latter isomer was more stable than the former, according to the NMR data and density functional theory (DFT) calculations. The title anion reacted with halide complexes of the type $[MXL_n]$ (ML_n = $FeCp(CO)_2$, $MoCp(CO)_3$, ZrCpCl, $Mn(CO)_5$, $Re(CO)_5$) to give compounds of formula $[Mo_2MCp_2(\mu\text{-}PCy_2)(\mu\text{-}\kappa^2\text{:}\kappa^2\text{:}\kappa^1\text{-}P_2)(CO)_2L_n]$ incorporating the organometallic fragment ML_n also in an "end-on" position at the basal P atom of the anion, as confirmed by the solid-state structure of the Fe compound (P−P = 2.089(2) Å; P−P−Fe = 124.6(1)°). All these complexes, except the Zr compound, underwent a fluxional process in solution involving a swing of the P_2 ligand around the Mo−Mo axis with concomitant exchange of the ML_n fragment between the P atoms of the diphosphorus ligand, as revealed by variable-temperature NMR experiments. Thermal decarbonylation of the Mn and Re compounds gave hexanuclear derivatives of formula $[Mo_4M_2Cp_4(\mu\text{-}PCy_2)_2(\mu_4\text{-}\kappa^1\text{:}\kappa^2\text{:}\kappa^2\text{:}\kappa^1\text{-}P_2)_2(CO)_{12}]$ (M = Mn, Re) as a mixture of two isomers derived from the different assembly of the asymmetric Mo_2P_2 subunits, as confirmed through X-ray analyses of both compounds. Each of the P_2 ligands in these two complexes bind two Mo and two M atoms (M = Mn, Re), with the latter defining central P_4M_2 six-membered rings with unusual boat conformations.

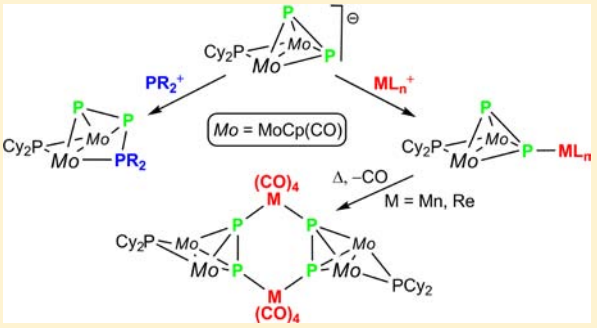

INTRODUCTION

Organometallic compounds with a "M_2P_2" tetrahedral core, that is, bearing a diphosphorus ligand symmetrically bridging a bonded dimetal unit, have been known for some 40 years now. The first example was described by Markó and co-workers, who reported the formation of the dicobalt complex $[Co_2(\mu\text{-}\kappa^2\text{:}\kappa^2\text{-}P_2)(CO)_6]$ from the reaction of the metal carbonylate $Na[Co(CO)_4]$ with PX_3 (X = Cl or Br).[1] However, the most common protocol to prepare such species is based on the symmetrical degradation of the white phosphorus molecule (P_4) mediated by dinuclear organometallic complexes, a reaction with low selectivity that usually takes place under harsh thermal or photochemical conditions.[2] Some reactivity studies have been also undertaken for these systems, most of them involving the addition of simple acceptor molecules, such as transition-metal moieties, although degradation and bond cleavage reactions are also known.[2] The addition reactions not leading to bond rupture in the M_2P_2 unit can be classified attending to the binding mode of the incoming fragment (Chart 1): The "end-on" types (**I** and **II** in Chart 1) involve the binding of the incoming metal fragment (M′) to one or both P atoms through the lone pairs (LP) of the latter;[3] the "side-on" type **III** involves the binding of the metal fragment at the P−P edge,[4] which is reminiscent of the addition of H^+ or Li^+ to the P_4 molecule, a reaction computed to occur preferentially at a P−P edge rather than at a P vertex;[5] more recently, complexes displaying "end-on"/"side-on" combinations (**IV** and **V**) have been also reported, these being prepared through the judicious choice of the reagents.[6]

Recently, we reported the symmetrical degradation of the P_4 molecule under mild conditions by the unsaturated anionic complex $[Mo_2Cp_2(\mu\text{-}PCy_2)(\mu\text{-}CO)_2]^-$ to give quantitatively the anionic derivative $[Mo_2Cp_2(\mu\text{-}PCy_2)(\mu\text{-}\kappa^2\text{:}\kappa^2\text{-}P_2)(CO)_2]^-$

Received: May 14, 2013
Published: July 9, 2013

   dx.doi.org/10.1021/ic401204j | Inorg. Chem. 2013, 52, 9005−9018

Chart 1

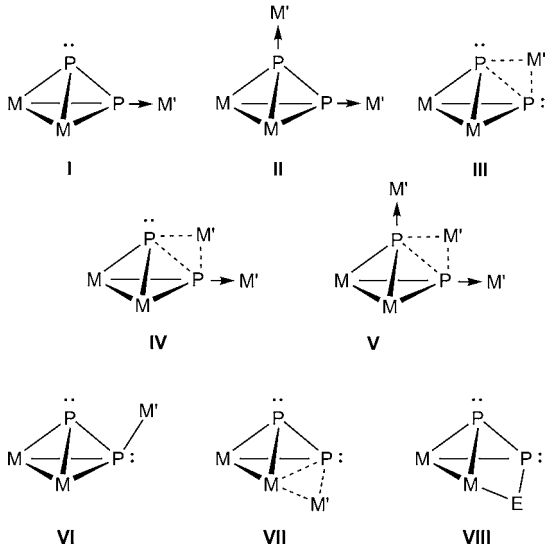

(**1**),[7] the first example of an anionic diphosphorus complex with a M_2P_2 tetrahedral core (Chart 2).[8] The reactivity of the

Chart 2

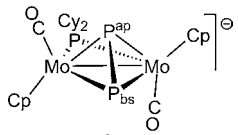

latter anion toward mild electrophiles based on elements of group 14 was explored in detail, and three different binding modes of the incoming fragment to the Mo_2P_2 unit were found, two of them unprecedented: (a) the already known "end-on" binding of type **I**, here involving a LP of the basal P atom (P^{bs} in Chart 2);[7] (b) a novel mode **VI** involving electron density located in a high-energy molecular orbital of **1** and having both σ(Mo−P) and π(P−P) bonding character, in which the incoming electrophile binds to the basal P atom in a position intermediate between those implied by the "end-on" and "side-on" modes, with P−P−M′ angles close to 90° (exemplified by the germanium and tin compounds $[Mo_2Cp_2(\mu\text{-}PCy_2)(\mu\text{-}\kappa^2\text{:}\kappa^2\text{-}P_2MPh_3)(CO)_2]$),[7b] and (c) another novel mode **VII**, in which the incoming electrophile binds to a basal Mo−P edge in a three-center−two-electron interaction, a mode also observed for the tin compound and computed to be the unique and most stable structure for the agostic-like diphosphenyl complex $[Mo_2Cp_2(\mu\text{-}PCy_2)(\mu\text{-}\kappa^2\text{:}\kappa^1,\eta^2\text{-}HP_2)(CO)_2]$.[7b]

Considering the novel structural features unveiled by the above reactions, it was of interest to examine the reactions of the anion **1** with other electrophiles based both on metal and nonmetal elements, so as to further explore the coordination ability of the Mo_2P_2 unit in this anion and to establish more general structural patterns. In this paper, we give a full account of the reactions of **1** with chlorophosphines PR_2Cl (R = Cy, Ph, ^{t}Bu), which mainly lead to the insertion of a PR_2^+ fragment in one of the Mo−P basal edges of **1**, to give unprecedented phosphinodiphosphenyl ligands. This can be considered as a novel variant of the binding possibilities of the M_2P_2 tetrahedron when faced with a carbene-like generic electrophile E^+ also bearing an electron pair (**VIII** in Chart 1). In contrast, the reactions of **1** with transition-metal halide complexes $[MXL_n]$ containing CO or Cp ligands or both ($[ZrCp_2Cl_2]$, $[MoICp(CO)_3]$, $[FeClCp(CO)_2]$, $[MnBr(CO)_5]$, and $[ReCl(CO)_5]$) always led to products of type **I**, which, however, displayed in most cases the exchange of the ML_n fragment between the P atoms of the diphosphorus ligands, a behavior thought previously to be exclusively associated with derivatives of **1** having structures of type **VI**.[7b] In addition, the Mn and Re complexes underwent further decarbonylation easily, then self-assembling to give derivatives with structures of type **II**, with both the apical and basal P atoms of the Mo_2P_2 tetrahedron bound to $M(CO)_4$ fragments via their LPs to define unusual six-membered P_4M_2 rings.

RESULTS AND DISCUSSION

Reactions of the Anion 1 with Chlorophosphines. Complex **1** reacts rapidly with different chlorophosphines PR_2Cl (R = Cy, Ph, ^{t}Bu) in tetrahydrofuran at room temperature. When R = Cy or Ph, these reactions gave selectively the corresponding phosphinodiphosphenyl complexes $[Mo_2Cp_2(\mu\text{-}PCy_2)(\mu\text{-}\kappa^2_{P,P'}\text{:}\kappa^2_{P,P''}\text{-}P_2PR_2)(CO)_2]$ (R = Cy (**2a**), Ph (**2b**)). However, the reaction with the bulkier phosphine P^tBu_2Cl led to a mixture of the isomers $[Mo_2Cp_2(\mu\text{-}PCy_2)(\mu\text{-}\kappa^2_{P,P'}\text{:}\kappa^2_{P,P''}\text{-}P_2P^tBu_2)(CO)_2]$ (**2c**) and $[Mo_2Cp_2(\mu\text{-}PCy_2)(\mu\text{-}\kappa^2_{P,P'}\text{:}\kappa^2_{P,P''}\text{-}P_2P^tBu_2)(CO)_2]$ (**3**), the latter having a pendant, noncoordinated P^tBu_2 group (Chart 3).

Chart 3

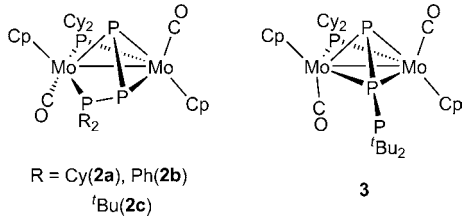

These isomers are in equilibrium in solution, with **3** being the major isomer at room temperature, according to the NMR data (see below). Moreover, small and variable amounts of the PH_2-bridged complex $[Mo_2Cp_2(\mu\text{-}PCy_2)(\mu\text{-}PH_2)(CO)_2]$ were obtained in all these reactions.[9] The latter was characterized by comparison of its IR and NMR spectroscopic data with those of previously reported complexes of the type $[Mo_2Cp_2(\mu\text{-}PR_2)(\mu\text{-}PHR')(CO)_2]$,[10] although deliberate procedures to prepare this side-product selectively (i.e., from the reaction of **1** with acids, water, or air) proved to be inefficient, and no further attempts to fully characterize this compound were made.

It is interesting to compare the above reactions of the anion **1** with those of white phosphorus with *in situ* generated PR_2^+ cations.[11] The latter reactions typically proceed via an electrophilic stage (electron donation from P_4 to the empty orbital of the cation: $P_4 \rightarrow PR_2$) followed by electronic rearrangement resulting in the insertion of the PR_2 group in a P−P bond (nucleophilic stage), to give cationic P_5 polyhedra.[12] Compound **3** nicely reproduces this first step, now taking place specifically at the basal P atom, and related species are likely to be formed in the reactions of **1** with PCy_2Cl and PPh_2Cl (not detected), which then rearrange rapidly by specific insertion in a Mo−P (rather than P−P) bond, to eventually give compounds **2**. We should also note that these reactions provide the first complexes having phosphinodiphosphenyl

dx.doi.org/10.1021/ic401204j | Inorg. Chem. 2013, 52, 9005−9018

ligands (P_2PR_2) that appear to have been described in the literature.

Solid-State Structure of Compound 2a. The structure of **2a** (Figure 1 and Table 1) can be viewed as derived from that

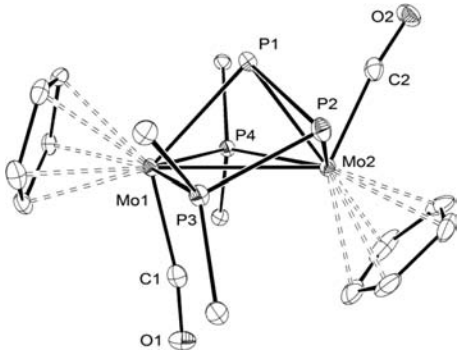

Figure 1. ORTEP diagram (30% probability) of compound **2a** with H atoms and Cy groups (except the C^1 atoms) omitted for clarity.

Table 1. Selected Bond Lengths (Å) and Angles (deg) for Compound 2a

Mo1−Mo2	3.0959(3)	Mo2−P1−Mo1	77.23(2)
P1−P2	2.185(1)	P1−P2−P3	83.01(4)
P2−P3	2.183(1)	P4−Mo1−P1	74.55(3)
Mo1−P1	2.5036(8)	P4−Mo1−P3	126.70(3)
Mo2−P1	2.4570(8)	C1−Mo1−Mo2	75.8(1)
Mo1−P4	2.4481(8)	C2−Mo2−Mo1	116.6(1)
Mo2−P4	2.4351(8)	C1−Mo1−P1	124.5(1)
Mo1−P3	2.5053(8)	C1−Mo1−P3	84.8(1)
Mo2−P2	2.5031(8)	C1−Mo1−P4	83.1(1)
Mo1−C1	1.957(3)	C2−Mo2−P1	70.3(1)
Mo2−C2	1.940(3)	C2−Mo2−P2	88.5(1)
		C2−Mo2−P4	95.0(1)

one computed for the anion **1** after insertion of a PCy_2^+ unit in a Mo−P^{bs} bond. This somehow distorts the Mo_2P_2 tetrahedral core, by removing one Mo−P bond (Mo1−P2) and establishing two new bonds, Mo1−P3 and P2−P3, (2.5053(8) and 2.183(1) Å respectively). The added phosphorus atom (P3) is located in the plane defined by the metal atoms and the μ-PCy_2 ligand, while the former "basal" P2 atom is shifted above that plane. Yet, the overall conformation of the molecule remains essentially unperturbed, with the Cp and CO ligands keeping a distorted transoid arrangement comparable to that in the anion **1**, with Mo−Mo−C(carbonyl) angles of 75.8(1)° and 116.6(1)°. This distortion minimizes the repulsion with the apical P atom (P1), which is located in the same plane as the average one defined by the $Mo_2(CO)_2$ unit. This geometrical feature is characteristic of different complexes of the type $[M_2Cp_2(\mu\text{-}PR_2)(\mu\text{-}X)(\mu\text{-}Y)(CO)_2]$ having three or more atoms bridging the dimetal unit.[7,13] The Mo1−P1 and Mo2−P1 lengths of 2.5036(8) and 2.4570(8) Å, respectively are slightly shorter than the corresponding lengths measured in the methyldiphosphenyl complex $[Mo_2Cp_2(\mu\text{-}PCy_2)(\mu\text{-}\kappa^2\text{:}\kappa^2\text{-}P_2Me)(CO)_2]$, a related molecule with an intact Mo_2P_2 tetrahedral core,[7] while the Mo2−P2 length of 2.5031(8) Å is significantly elongated (by ca. 0.1 Å). Perhaps, the most significant change takes place in the P−P distance within the P_2 unit, now closer to a normal single P−P bond (2.185(1) Å vs 2.21 Å measured for the P_4 molecule) and significantly longer (by ca. 0.1 Å) than the one computed for the parent anion **1** or that measured for the mentioned methyldiphosphenyl complex (2.085(1) Å). This can be attributed to the almost complete absence of any residual π(P−P) interaction in that bond of compound **2a**. Actually, the single bond connecting the P2 and P3 atoms in **2a** has an almost identical length of 2.183(1) Å.

Compound **2a** appears to be the first complex with a phosphinodiphosphenyl ligand (P_2PR_2) to be structurally characterized. Actually, to the best of our knowledge no other complex with this sort of ligand seems to have been ever reported. The $\mu\text{-}\kappa^2_{P,P'}\text{:}\kappa^2_{P,P''}$-coordination mode observed for **2a**, however, can be related to those found for some phosphinodiphosphene-bridged complexes[14] and also to that in the phosphine−diphosphorus-bridged CoPt complex $[CoPt(\mu\text{-}P_2PPh_2CH_2PPh_2)_2(PPh_3)_2]BF_4$.[15]

Solution Structure of Compounds 2a−c and 3. The IR spectra of compounds **2a** and **2b** in the C−O stretching region display two bands around 1850 cm^{-1} (Table 2) with relative intensities (medium and strong, in order of decreasing frequencies) characteristic of complexes having transoid $M_2(CO)_2$ oscillators defining an obtuse angle between both CO ligands (ca. 140° for **2a** in the crystal).[16] As expected on electronic grounds, the bands of the PPh_2 derivative (**2b**) are shifted to frequencies higher than the corresponding ones in the PCy_2 compound (**2a**). On the other hand, the IR spectrum of the mixture of isomers **2c** and **3** also displays two bands, obviously corresponding to the major isomer **3**, which are less energetic than those of the above complexes, as anticipated from the stronger donor properties of the P^tBu_2 group.

The $^{31}P\{^1H\}$ NMR spectra of compounds **2a−c** in CD_2Cl_2 solution at room temperature exhibit in each case a singlet at ca. 150 ppm attributed to the bridging PCy_2 ligand, as well as three resonances corresponding to the phosphinodiphosphenyl ligand. The resonance for the P^{bs} atom is easily identified as the only one exhibiting two large one-bond P−P couplings around 250 Hz (δ ca. +20 to −20 ppm), while the one arising from the added PR_2 group is identified as the only one being modified upon ^1H coupling, it appearing within the same range of shifts. The third resonance therefore is assigned to the apical P^{ap} atom and appears as the most deshielded one in all cases (δ ca. +50 to +75 ppm). We note that the absolute one-bond P−P couplings measured for **2a−c** fall in the range of values found for diphosphines of formula RR′P−PR″$_2$ (R, R′, R″ = Me, Et, ^{i}Pr, Ph, or ^{t}Bu).[17] Moreover, the DFT-computed figures for compound **2c** (−361 and −344 Hz for P^{ap}−P^{bs} and P^{bs}−P^tBu_2, respectively, Table 3) reproduce the relative magnitude of the experimental figures (286 and 256 Hz, respectively), while the negative sign of these one-bond couplings can be attributed to the presence of lone pairs at both the P^{ap} and P^{bs} atoms.[18] Other spectroscopic data of compounds **2** (^1H, ^{13}C NMR, see the Experimental Section) are in agreement with their asymmetric structures and deserve no particular comments.

The $^{31}P\{^1H\}$ NMR spectrum of **3** at room temperature displays resonances quite different from those of its isomer **2c**, consistent with a structure of type **I** (Chart 1) similar to that of the methyldiphosphenyl complex $[Mo_2Cp_2(\mu\text{-}PCy_2)(\mu\text{-}\kappa^2\text{:}\kappa^2\text{-}P_2Me)(CO)_2]$.[7] The P^{ap} and P^{bs} atoms now appear much more shielded (at ca. −180 ppm) and strongly coupled to each other (446 Hz); for comparison, the corresponding resonances in the above methyldiphosphenyl complex appear at −293 and −84 ppm (J_{PP} = 503 Hz). Unexpectedly, the chemical shift of the pendant P^tBu_2 group of **3** is comparable to that in its isomer **2c**, despite the dramatic difference in the corresponding P environments. Moreover, its coupling to the basal P atom

dx.doi.org/10.1021/ic401204j | Inorg. Chem. 2013, 52, 9005−9018

Table 2. Selected IR[a] and $^{31}P\{^1H\}$ NMR Data[b] for New Compounds

compound	ν(CO)	$\delta(\mu$-P)	$\delta(P^{ap})$	$\delta(P^{bs})$	$\delta(PR_2)$	$J(P^{ap}P^{bs})$	$J(P^{bs}PR_2)$
$[Mo_2Cp_2(\mu\text{-}PCy_2)(\mu\text{-}\kappa^2_{P,P'}\text{:}\kappa^2_{P,P''}\text{-}P_2PCy_2)(CO)_2]$ (**2a**)	1859 (m, sh), 1836 (vs)	154.5	74.8	−6.3	−19.6	277	229
$[Mo_2Cp_2(\mu\text{-}PCy_2)(\mu\text{-}\kappa^2_{P,P'}\text{:}\kappa^2_{P,P''}\text{-}P_2PPh_2)(CO)_2]$ (**2b**)	1873 (s, sh), 1856 (vs)	149.8	71.9	18.8	−25.0	270	252
$[Mo_2Cp_2(\mu\text{-}PCy_2)(\mu\text{-}\kappa^2_{P,P'}\text{:}\kappa^2_{P,P''}\text{-}P_2P^tBu_2)(CO)_2]$ (**2c**)	1866 (s), 1825 (vs)[c]	144.6[d]	50.2	−23.6	18.2	286	256
$[Mo_2Cp_2(\mu\text{-}PCy_2)(\mu\text{-}\kappa^2_{P,P'}\text{:}\kappa^2_{P,P'}\text{-}P_2P^tBu_2)(CO)_2]$ (**3**)		149.2[d]	−184.1	−168.4	47.9	446	446
$[Mo_2FeCp_3(\mu\text{-}PCy_2)(\mu_3\text{-}\kappa^2\text{:}\kappa^2\text{:}\kappa^1\text{-}P_2)(CO)_4]$ (**4**)	2025 (vs), 1982 (s), 1854 (m), 1803 (m)	162.3[d,e]	−228.9	−53.5		491	
$[Mo_3Cp_3(\mu\text{-}PCy_2)(\mu_3\text{-}\kappa^2\text{:}\kappa^2\text{:}\kappa^1\text{-}P_2)(CO)_5]$ (**5**)	2019 (vs), 1956 (s, sh), 1942 (s), 1857 (m), 1812 (m)	158.3[d,f]	−191.8	−134.8		480	
$[Mo_2ZrClCp_4(\mu\text{-}PCy_2)(\mu_3\text{-}\kappa^2\text{:}\kappa^2\text{:}\kappa^1\text{-}P_2)(CO)_2]$ (**6**)	1892 (m), 1852 (vs)	143.2[d]	−320.3	−129.7		460	
$[Mo_2MnCp_2(\mu\text{-}PCy_2)(\mu_3\text{-}\kappa^2\text{:}\kappa^2\text{:}\kappa^1\text{-}P_2)(CO)_7]$ (**7**)	2108 (w), 2023 (m), 1895 (m), 1862 (vs)[g]	155.6	−168.4 (br)				
$[Mo_2ReCp_2(\mu\text{-}PCy_2)(\mu_3\text{-}\kappa^2\text{:}\kappa^2\text{:}\kappa^1\text{-}P_2)(CO)_7]$ (**8**)	2130 (m), 2030 (vs), 1997 (m), 1863 (w), 1809 (w)	154.8[d,h]	−200.8	−256.6(br)		460	
$[Mo_4Mn_2Cp_4(\mu\text{-}PCy_2)_2(\mu_4\text{-}\kappa^1\text{:}\kappa^2\text{:}\kappa^2\text{:}\kappa^1\text{-}P_2)_2(CO)_{12}]$ (**9R**)	2062 (s), 2001 (sh)[i]	165.2	−184.0 (br)				
$[Mo_4Mn_2Cp_4(\mu\text{-}PCy_2)_2(\mu_4\text{-}\kappa^1\text{:}\kappa^2\text{:}\kappa^2\text{:}\kappa^1\text{-}P_2)_2(CO)_{12}]$ (**9M**)	2075 (w), 2067 (vs), 2011 (s), 1989 (vs), 1974 (sh), 1961 (sh), 1888 (w), 1827 (w)	164.3	−184.5 (br)				
$[Mo_4Re_2Cp_4(\mu\text{-}PCy_2)_2(\mu_4\text{-}\kappa^1\text{:}\kappa^2\text{:}\kappa^2\text{:}\kappa^1\text{-}P_2)_2(CO)_{12}]$ (**10R**)	2097 (w), 2085 (m), 2012 (vs), 1988 (s), 1858 (s), 1888 (w), 1822 (w)[j]	161.7	−276.0 (br)				
$[Mo_4Re_2Cp_4(\mu\text{-}PCy_2)_2(\mu_4\text{-}\kappa^1\text{:}\kappa^2\text{:}\kappa^2\text{:}\kappa^1\text{-}P_2)_2(CO)_{12}]$ (**10M**)		160.9	−276.0 (br)				

[a]Recorded in dichloromethane solution with C−O stretching bands [ν(CO)] in cm^{-1}. [b]Recorded in CD_2Cl_2 at 121.50 MHz and 298 K, with coupling constants (J_{PP}) in Hz; P^{ap} and P^{bs} refer to the "apical" and "basal" P atoms of the Mo_2P_2 tetrahedron (see Chart 2). [c]IR spectrum for the equilibrium mixture of isomers (**3**/**2c** ca. 7). [d]At 161.98 MHz. [e]At 238 K. [f]At 240 K. [g]In tetrahydrofuran. [h]At 198 K. [i]The rest of the bands could not be unambiguously assigned due to overlapping with those of the isomer **9M**. [j]IR spectrum of a ca. 1:1 mixture of isomers **10R** and **10M**.

Table 3. Selected DFT-Computed ^{31}P NMR Parameters for Compounds 2c, 3, and 4A[a]

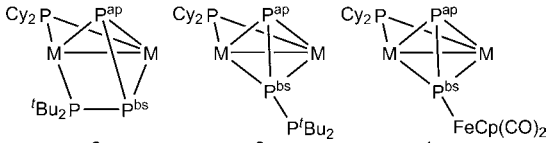

2c **3** **4**

	2c	3	4A
$\delta(\mu$-P)	149.1	149.3	161.9
$\delta(P^{ap})$	154.7	−166.6	−187.0
$\delta(P^{bs})$	8.8	−153.2	−55.6
$\delta(P^tBu_2)$	9.4	16.8	
$J(P^{ap}-P^{bs})$	−361	−519	−548
$J(P^{bs}-P^tBu_2)$	−344	−582	

[a]Values in ppm for the DFT-optimized structures, with the labeling scheme shown in the structures. Chemical shifts (δ) are given so as to fit the computed value of $\delta(\mu$-$PCy_2)$ of compound **4A** to the experimental figure of 161.9 ppm, and coupling constants (J) are given in hertz.

(446 Hz) is unusually large for a single-bond P−P coupling, an effect that we can attribute to the negative contribution provided now by the lone pair at this pendant P^tBu_2 group.[18] Indeed, the DFT-computed NMR parameters for a type **I** structure for compound **3** reproduced well these experimental spectroscopic properties (Table 3), that is, a chemical shift for the P^tBu_2 group comparable to that in **2c** but with a largely increased P−P coupling (−582 vs −344 Hz), the latter in turn having a value comparable to the $P^{ap}-P^{bs}$ coupling (−519 Hz), while the P^{ap} and P^{bs} atoms become strongly but similarly shielded (ca. −150 ppm).

As noted above, the phosphinodiphosphenyl isomers **2c** and **3** are in equilibrium, with the latter being dominant at room temperature. The **3**/**2c** ratio was ca. 7 both in CD_2Cl_2 and toluene-d_8 solutions, as determined from the corresponding ^1H NMR spectra, but the relative amount of **2c** increased at lower temperatures to reach ratios of ca. 8:5 at 253 K and ca. 4:5 at 213 K (toluene-d_8 solutions). From these data, it can be concluded that the energy of both isomers is similar, despite their significant structural differences, a conclusion supported by the calculations discussed below.

DFT-Optimized Structures of Isomers 2c and 3. As noted above, the proposed structure of type **I** for the isomer **3** reproduces the structure of the intermediate species following from the electrophilic stage that initiates the activation of the P_4 molecule by different main-group based electrophiles.[11] It was therefore of interest confirming that the geometry of this molecule indeed falls into this structural category, rather than other alternatives (e.g., structures of type **VI**). To accomplish this, we carried out Density Functional theory (DFT) calculations on both isomers **2c** and **3** (see the Experimental Section and Supporting Information for details).[19]

The optimized geometry of **2c** (Figure 2 and Table 4) is in general very similar to the one experimentally determined for the P_2PCy_2 complex **2a**, although the computed values for distances involving the metal atoms are a bit longer than the experimental figures, which is a common trend observed with the functionals currently used in the DFT computations of transition metal compounds.[19a,20] However, the computed Mo−P^tBu_2 length of 2.664 Å is significantly longer than the corresponding Mo−PCy_2 length of 2.5031(8) Å in **2a**, which we interpret as a clear reflection of the great steric pressure induced by the bulky P^tBu_2 group over this structure. The latter should have a destabilizing effect on the complex, thus

dx.doi.org/10.1021/ic401204j | Inorg. Chem. 2013, 52, 9005−9018

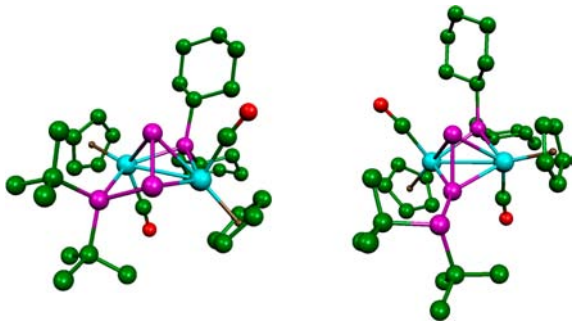

Figure 2. DFT-optimized structure of isomers **2c** (left) and **3** (right), with H atoms omitted for clarity.

Table 4. Selected Bond Lengths (Å) and Angles (deg) Computed for Isomers 2c and 3[a]

param	2c	3
Mo−Mo	3.148	3.058
Mo1−P^{ap}	2.566	2.575
Mo2−P^{ap}	2.480	2.522
Mo1−P^{bs}		2.497
Mo2−P^{bs}	2.575	2.508
Mo1−P^tBu_2	2.664	
P^{ap}−P^{bs}	2.208	2.120
P^{bs}−P^tBu_2	2.239	2.243
P^{ap}−P^{bs}−P^tBu_2	84.7	114.7

[a]Labeling according to the figures in Table 3

explaining the lower stability of **2c** over its isomer **3**, where the bulky P^tBu_2 group points away from the rest of the molecule. Indeed, the Gibbs free energy computed for **2c** at 295 K in toluene solution is some 25 kJ/mol above that of **3**, with this difference being reduced by some 5 kJ/mol at 183 K, in qualitative agreement with the experimental data discussed above.

The optimized geometry of **3** (Figure 2 and Table 4) belongs to the structural type **I** and displays metric parameters comparable to those computed and measured for the methyldiphosphenyl complex $[Mo_2Cp_2(\mu\text{-}PCy_2)(\mu\text{-}\kappa^2\text{:}\kappa^2\text{-}P_2Me)(CO)_2]$:[7] a quite short P^{ap}−P^{bs} length (2.120 Å), a P^{ap}−P^{bs}−electrophile angle close to 120° (114.7°) and relatively short Mo−P^{bs} lengths (ca. 2.50 Å). This is accompanied by the retention of large P^{ap}−P^{bs} couplings (computed value −519 Hz), as noted above.

Reactivity of the Anion 1 with Transition-Metal Halide Complexes. The addition of different transition-metal halide complexes $[MXL_n]$ to tetrahydrofuran solutions of the Li^+ salt of the anion **1** leads to the facile incorporation of organometallic fragments ML_n to the P^{bs} atom of the P_2 ligand in an "end-on" position, to give μ_3-P_2 heterometallic derivatives with structures of type **I** rather than **VI** (Chart 1). Thus the reactions with $[FeClCp(CO)_2]$, $[MoCpI(CO)_3]$, $[ZrCl_2Cp_2]$, $[MnBr(CO)_5]$, and $[ReCl(CO)_5]$ gave the corresponding derivatives $[Mo_2MCp_2(\mu\text{-}PCy_2)(\mu\text{-}\kappa^2\text{:}\kappa^2\text{:}\kappa^1\text{-}P_2)(CO)_2L_n]$ (ML_n = $FeCp(CO)_2$ (**4**), $MoCp(CO)_3$ (**5**), $ZrCp_2Cl$ (**6**), $Mn(CO)_5$ (**7**), $Re(CO)_5$ (**8**), respectively, see Chart 4). These reactions could be carried out conveniently at room temperature in short times (ca. 15 min), except for compounds **5** and **7**, which were better prepared at temperatures below 273 K to avoid undesired side reactions (**5**) or further decarbonylation (**7**, see below). Once more, all these reactions also yielded small

Chart 4

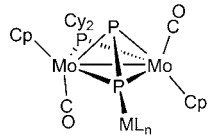

	M	L_n
4	Fe	$Cp(CO)_2$
5	Mo	$Cp(CO)_3$
6	Zr	Cp_2Cl
7	Mn	$(CO)_5$
8	Re	$(CO)_5$

amounts of the PH_2-bridged byproduct $[Mo_2Cp_2(\mu\text{-}PCy_2)(\mu\text{-}PH_2)(CO)_2]$, which could be easily separated from the main product through column chromatography except for compound **6**, itself unstable in alumina, which was instead purified through selective extraction with petroleum ether.

Solid-State Structure of Compound 4. The molecule of **4** in the crystal (Figure 3 and Table 5) is built from two

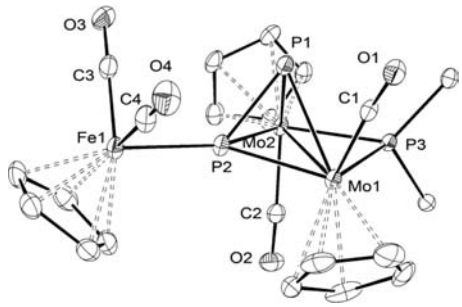

Figure 3. ORTEP diagram (30% probability) of compound **4** with H atoms and Cy groups (except the C^1 atoms) omitted for clarity.

Table 5. Selected Bond Lengths (Å) and Angles (deg) for Compound 4

Mo1−Mo2	3.0077(6)	C1−Mo1−Mo2	114.6(2)
P1−P2	2.089(2)	C2−Mo2−Mo1	78.1(2)
Fe1−P2	2.262(2)	P1−P2−Fe1	124.6(1)
Mo1−P1	2.506(2)	Mo2−P1−Mo1	73.3(1)
Mo2−P1	2.534(2)	Mo1−P2−Mo2	76.1(1)
Mo1−P2	2.434(2)	C1−Mo1−P1	66.2(2)
Mo2−P2	2.445(2)	C1−Mo1−P2	104.5(2)
Mo1−P3	2.454(2)	C1−Mo1−P3	97.7(2)
Mo2−P3	2.433(2)	C2−Mo2−P1	127.9(2)
Mo1−C1	1.936(6)	C2−Mo2−P2	86.4(2)
Mo2−C2	1.949(6)	C2−Mo2−P3	87.0(2)
Fe1−C3	1.775(7)	C3−Fe1−P2	86.9(2)
Fe1−C4	1.778(7)	C4−Fe1−P2	87.3(2)

MoCp(CO) fragments in a transoid arrangement and bridged symmetrically by PCy_2 and diphosphorus (P_2) ligands. The resulting Mo_2P_2 core displays a tetrahedral geometry as in the parent anion,[7] and it is bound to a $FeCp(CO)_2$ moiety through a single bond via the basal P atom, as denoted by the Fe1−P2 length of 2.262(2) Å. In essence, the structure of **4** is closely reminiscent of the type **I** structure displayed by the methyldiphosphenyl complex mentioned above,[7a] implying that the Fe atom is roughly located on the average plane defined by the Mo, P2, and P3 atoms. As a result, the Fe1−P2−P1 angle (124.6(1)°) must be close to the figure of 120°, (cf. 122.8(1)° for the P_2C angle in the methyldiphosphenyl complex). The Cp and CO ligands bound to each Mo atom exhibit a distorted transoid arrangement analogous to that in **2a**, with one carbonyl leaning toward the intermetallic bond (M−M−C = 78.1(2)°) and the other one pointing away from

dx.doi.org/10.1021/ic401204j | Inorg. Chem. 2013, 52, 9005−9018

Scheme 1. Fluxional Process Proposed for Compounds 4, 5, 7, and 8 in Solution

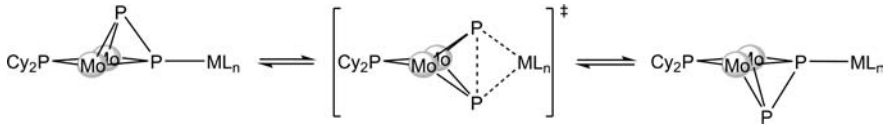

it (M−M−C = 114.6(2)°), to avoid the close apical P atom of the diphosphorus ligand. Finally, the P−P distance in the latter ligand (2.089(2) Å) remains quite short, definitely shorter than expected for a single bond (ca. 2.18 Å in compound **2a**) and comparable again with that in the methyldiphosphenyl complex (2.095(1) Å), an experimental figure that we have interpreted as indicative of the retention of some π(P−P) contribution to this bond.[7]

Solution Structure of Compounds 4 and 5. The IR spectrum of **4** in dichloromethane solution displays four bands in the C−O stretching region, which can be viewed as arising from independent $Fe(CO)_2$ and $Mo_2(CO)_2$ oscillators: the two low-frequency bands (1854 and 1803 cm^{-1}) compare well with those of the mentioned μ-P_2Me complex, and can therefore be assigned to the latter oscillator, whereas the bands of similar relative intensity at 2025 and 1981 cm^{-1} can be safely assigned to the $Fe(CO)_2$ moiety.[16] Analogously, the corresponding bands in the IR spectrum of compound **5** can also be viewed as arising from two independent oscillators, now $Mo(CO)_3$ and $Mo_2(CO)_2$ ones. As expected, the former gives rise to three intense bands around 2000 cm^{-1}, and the latter generates two bands at lower frequencies, with pattern and frequencies similar to those of the $Mo_2(CO)_2$ oscillator in the iron complex **4**.

Although the structure of compounds **4** and **5** can be related to that of the mentioned μ-P_2Me complex, a fundamental difference is found in their dynamic behavior. Thus, whereas the latter complex and its P_2CH_2Ph analogue were found to be rigid on the NMR time scale,[7] compounds **4** and **5** (and also **7** and **8**, see below) exhibit a dynamic behavior previously observed only for type **VI** derivatives of the anion **1** such as the compounds $[Mo_2Cp_2(\mu\text{-}\kappa^2\text{:}\kappa^2\text{-}P_2MPh_3)(\mu\text{-}PCy_2)(CO)_2]$ (M = Ge, Sn, Pb).[7b] Thus, the $^{31}P\{^1H\}$ NMR spectrum of **4** at room temperature displays a triplet at 161.9 ppm (J_{PP} = 12 Hz) corresponding to the bridging PCy_2 ligand, and two broad resonances at ca. −50 and ca. −220 ppm corresponding to the P_2 unit, which can be assigned to the basal and apical P atoms, respectively, on the basis of our DFT calculations (computed values −55.6 and −187.0 ppm, Table 3) and their distinct behavior at lower temperatures. Upon cooling of the solution these two signals sharpen, and at 238 K, they appear as strongly coupled doublets (J_{PP} = 491 Hz; computed value −548 Hz) at −53.2 and −228.8 ppm, which seems to be a spectroscopic feature characteristic of type **I** derivatives of the anion **1**.[7b] The fluxional process responsible for this broadening must be essentially identical to that observed and computed for the mentioned type **VI** complexes $[Mo_2Cp_2(\mu\text{-}\kappa^2\text{:}\kappa^2\text{-}P_2MPh_3)(\mu\text{-}PCy_2)(CO)_2]$[7b] and would involve the swing of the P_2 unit around the Mo−Mo axis with concomitant exchange of the metallic fragment between the P atoms (Scheme 1). In fact, this sort of dynamic process would be also operative for compounds **5**, **7**, and **8**, as discussed later on. We also note that the proposed dynamic process is comparable to the "pendulum motion" of the Ru fragment recently reported for several P_4-bridged RuPt complexes.[21] Upon further cooling to 178 K, a splitting of the basal P resonance of **4** was observed, which we attribute to the presence in solution of a minor rotamer having a different orientation of the $FeCp(CO)_2$ fragment with respect to the Mo_2P_2 tetrahedron. Indeed we have found that, in addition to the conformation found in the solid state (**4A**), a second structure **4B**, obtained by rotating the $FeCp(CO)_2$ fragment by ca. 120° around the Fe−P axis, is a true minimum in the potential energy surface of the compound, and is placed only ca. 3 kJ/mol above the major isomer **4A** in the gas phase (see the Supporting Information). From these calculations, we can safely conclude that, despite its dynamic behavior, compound **4** retains in solution a structure of type **I** under all circumstances. Apparently, any structure of type **VI** is strongly disfavored here (as it is the case of compounds **5**−**8**) surely on steric reasons, in line with our previous conclusions on the relative stability of these two types of structures in the group 14 derivatives of the anion **1**.[7b]

The ^1H and $^{13}C\{^1H\}$ NMR spectra of **4** are also consistent with the proposed dynamic process in solution, as the room temperature spectra display averaged resonances for the pairs of Cy and Mo-bound Cp and CO groups. On cooling of the solutions to 198 K, all these resonances split in agreement with the static structure of the complex. Thus, the Mo-bound Cp ligands give rise to separate ^1H and ^{13}C NMR resonances, and the CO ligands give rise to four independent resonances at 241.3 (d, J_{CP} = 35, MoCO), 238.4 (br, MoCO), 213.9 (d, J_{CP} = 16, FeCO), and 213.1 ppm (d, J_{CP} = 20, FeCO). From the coalescence temperature of 208 K for the proton Cp resonances, we can estimate a Gibbs free energy of ca. 47 ± 1 kJ/mol for the corresponding activation barrier,[22] which is somewhat higher than the values of ca. 35−40 kJ/mol measured for the type **VI** compounds $[Mo_2Cp_2(\mu\text{-}\kappa^2\text{:}\kappa^2\text{-}P_2MPh_3)(\mu\text{-}PCy_2)(CO)_2]$ (M = Ge, Sn Pb),[7b] but lower than the values of 55−61 kJ/mol determined for the mentioned P_4-bridged RuPt complexes.[21] The difference with compounds of type **VI** is not unexpected, since type **VI** derivatives of **1** are along the rearrangement coordinate of fluxional structures of type **I** but not *vice versa*. We finally note that the different P−C couplings observed for the CO ligands of **4** can be easily explained by recalling the progressive reduction in the absolute $^2J_{CP}$ values usually observed in this sort of molecules upon increasing the C−M−P angles.[18,23] Thus, the downfield resonance with the largest coupling is assigned to the CO ligand *cis* to the axial P atom (C1−Mo1−P1 = 66°) while the other Mo-bound carbonyl displays larger angles and hence small couplings. In contrast, the Fe-bound carbonyls display P−C couplings to the P^{bs} atom similar to each other (16 and 20 Hz), in agreement with their similar C−Fe−P angles (ca. 87°). Interestingly, although the dynamic process does not average the chemical shifts of the Fe-bound carbonyls, it does average their coupling to the diphosphorus atoms, since at room temperature these carbonyls appear as triplets with halved couplings (8 and 10 Hz). This can be explained by considering the expected negligible value of the tree-bond C−P^{ap} coupling, and in any case, it proves that the undergoing dynamic process is intramolecular.

The $^{31}P\{^1H\}$ NMR spectrum of **5** at room temperature displays a triplet resonance at 157.9 ppm (J_{PP} = 13 Hz)

dx.doi.org/10.1021/ic401204j | Inorg. Chem. 2013, 52, 9005−9018

corresponding to a PCy_2 group equally coupled to both atoms of the diphosphorus ligand. The resonances of the latter, however, were not observed, suggesting that at room temperature we are close to the coalescence temperature for a dynamic process that averages the P^{bs} and P^{ap} environments, as proposed for **4**. Indeed, after cooling to 270 K, two broad resonances are observed at −134.8 and −188.2 ppm, which at 240 K already appear as strongly coupled doublets (480 Hz), as expected for a type **I** derivative of the anion **1**. The ^1H NMR spectra of **5** are also consistent with this process, as the singlet (δ 5.20 ppm) observed at room temperature for both Mo-bound Cp groups splits into well separate resonances at 208 K (δ 5.28 and 5.17 ppm). From the corresponding coalescence temperature of 245 K, we can estimate a value of 50 ± 1 kJ/mol for the Gibbs free energy of the corresponding activation barrier,[22] which is somewhat higher than that for **4**, in agreement with the mass differences of the migrating metal fragments involved.

Solution Structure of Compound 6. The IR spectrum of **6** displays two C−O stretches at 1892 (m) and 1852 (vs) cm^{-1} denoting a distorted transoid arrangement of the CO ligands of the molecule, as found in all derivatives of **1** described so far. We note, however, that these bands are some 40 cm^{-1} more energetic than those of compounds **4** or **5**, which is a reflection of the higher electron-withdrawing character of the Zr(IV) center compared with the Mo(II) or Fe(II) centers attached to the Mo_2P_2 tetrahedron in the above compounds. Another difference with respect to these species lies in the fact that **6** behaves as a rigid molecule on the NMR time scale at room temperature. Thus its $^{31}P\{^1H\}$ NMR spectrum at room temperature displays two well-resolved doublets at −129.7 and −320.3 ppm, attributed to the basal (P−Zr) and apical P atoms, respectively, with the large one-bond P−P coupling (463 Hz) characteristic of all type **I** derivatives of the anion **1**. At the same time, its ^1H NMR spectrum displays separate resonances for the Cp ligands attached to Zr (δ_H 6.49 and 6.30 ppm), and for those attached to Mo atoms (δ_H 5.17 and 5.02 ppm), this being also consistent with the static structure of the molecule.

Solution Structure of Compounds 7 and 8. The spectroscopic data in solution for compounds **7** and **8** are similar to each other, indicating that they share the same structural features, in turn comparable to those of compounds **4**−**6** discussed above. Data for compound **7**, however, could only be obtained from impure samples of this complex, which we could not further purify, and were thus incomplete.

The IR spectrum of the rhenium complex **8** displays five bands within the C−O stretching region; the three bands at high frequencies (2131 (w), 2031 (vs) and 1997 (m) cm^{-1}) have the pattern characteristic of pentacarbonyl complexes of the type $XM(CO)_5$,[16] and therefore are assigned to the active C−O stretching modes arising from the $Re(CO)_5$ oscillator of the molecule. The two bands at lower frequency are comparable to those observed for compounds **4**−**6**, and are then assigned to the C−O stretches of the transoid $Mo_2(CO)_2$ oscillator. We can take the average frequency of the latter two bands as an indicator of the electron-density withdrawal from the Mo_2 center of **1** by the added ML_n^+ fragment, this rendering the sequence **6** (1872 cm^{-1}) > **8** (1836 cm^{-1}) ≥ **5** (1835 cm^{-1}) > **4** (1829 cm^{-1}), which reveals the expected trends, that is, a stronger withdrawal power of the fragments having higher oxidation states (Zr(IV)) and a larger number of CO ligands (Re > Mo > Fe, despite the oxidation states Mo(II) = Fe(II) > Re(I)).

The $^{31}P\{^1H\}$ NMR spectra of compounds **7** and **8** at room temperature in CD_2Cl_2 solution reveal the operation of dynamic processes reminiscent of those proposed for compounds **4** and **5** (Scheme 1) but even faster ones: in both cases the P_2 ligand gives rise at room temperature to a single and broad upfield resonance, at −168.4 (**7**) and −220.7 ppm (**8**). This fluxional process was analyzed in more detail for the more stable Re complex: upon cooling the solution, the diphosphorus resonance eventually split to yield two broad lines at −203.4 and −255.3 ppm at 238 K, which further sharpened at 198 K, then appearing as strongly coupled doublets (δ −200.8 and −256.6 ppm, J_{PP} = 460 Hz), as expected for a type **I** derivative of the anion **1**. The most shielded resonance was significantly broader, perhaps denoting slow rotation of the $Re(CO)_5$ fragment around the $Re-P^{bs}$ bond as found for **4**, and therefore was assigned to the P^{bs} atom of the diphosphorus ligand. Indeed, further broadening was observed on cooling at 173 K, although no additional splitting of this resonance occurred yet at this point.

The ^1H NMR spectra of compounds **7** and **8** at room temperature also are indicative of fluxional behavior, since both complexes display just a single and broad resonance at ca. 5.20 ppm for the Cp ligands. Upon cooling, the resonance of the Re complex further broadened and eventually split to give at 173 K well-separated resonances at 5.22 and 5.20 ppm. From the corresponding coalescence temperature (T_c = 182 K), we can estimate a value of 39 ± 1 kJ/mol for the pertinent activation barrier,[22] a figure somewhat lower than those measured for the Fe and Mo compounds discussed above. Analogous modifications were observed in the $^{13}C\{^1H\}$ NMR spectra of **8**: at room temperature, averaged resonances for the Cp and CO ligands were observed, while at 183 K separate resonances were observed for all these ligands, as expected for a complex with no symmetry elements. For instance, the Mo-bound CO ligands now gave rise to a strongly coupled doublet at 240.7 ppm (J_{CP} = 34 Hz), similar to that found for the Fe complex **4** and analogously assigned to the carbonyl positioned cis to the P^{ap} atom, and a singlet at 237.5 ppm. At that temperature, the Re-bound carbonyls gave rise to two signals, a broad and intense one at 182.3 ppm corresponding to the four equatorial ligands and a doublet at 177.1 ppm (J_{CP} = 31 Hz), which can be safely assigned to the axial carbonyl.

^{31}P NMR Trends in μ-P_2 Complexes. In our previous study on the group 14 derivatives of the anion **1**, we found that variations in the chemical shifts of the diphosphorus resonances were largely dominated by the paramagnetic contribution to the shielding of the P nuclei and were also critically dependent on the structure of the molecule (type **I** vs type **VI** structures), so that type **I** structures were characterized by strongly shielded P^{ap} resonances and relatively deshielded P^{bs} resonances, whereas the reverse applied for structures of type **VI**.[7b] Now the data on compounds **4**−**8** and the computed NMR parameters for **4** (Table 3 and Supporting Information) indicate that these trends also hold for transition-metal derivatives of the anion **1** with structures of type **I**. In fact, the resonances for P^{ap} in compounds **4**−**8** are found at ca. −200 ppm except for the Zr compound **6**, significantly more shielded (δ −320.3 ppm) without obvious reason. As expected, the resonance for the basal P atom displays a marked influence of the metal bound to it, with the heavier atoms yielding the

dx.doi.org/10.1021/ic401204j | Inorg. Chem. 2013, 52, 9005−9018

Chart 5

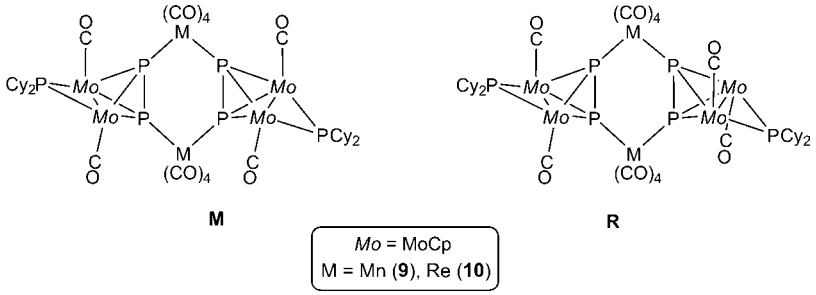

less deshielded resonances (δ in the order Re < Mo ≤ Zr < Fe), as usually observed for metal-bound P atoms of any type.

Decarbonylation of Compounds 7 and 8. As noted above, decarbonylation of the Mn derivative **7** takes place during attempted chromatographic purification of the crude reaction mixtures on alumina columns, thus hindering its isolation as a pure species, and also takes place when tetrahydrofuran solutions of the complex are stirred at room temperature. The process involves the release of a molecule of CO from the $Mn(CO)_5$ fragment of the complex and the self-assembly of two resulting units via the nucleophilic attack by the LP of the P^{ap} atom in one molecule to the unsaturated $Mn(CO)_4$ fragment of another one and *vice versa*, thus yielding the hexanuclear complex $[Mo_4Mn_2Cp_4(\mu\text{-}PCy_2)_2(\mu_4\text{-}\kappa^1\text{:}\kappa^2\text{:}\kappa^2\text{:}\kappa^1\text{-}P_2)_2(CO)_{12}]$ (**9**) having a central Mn_2P_4 ring. The above dimerization can lead to two possible isomers, depending whether the involved subunits are the same or different optical isomer. In the first case, a symmetrical (C_2) isomer results (**9R** in Chart 5), whereas a fully asymmetrical isomer is formed in the second instance (**9M**). We found no evidence of interconversion between these isomers, which were obtained usually in a **9R**/**9M** ratio of ca. 3/2 under the above experimental conditions and could not be separated chromatographically. The isomer **9M**, however, could be obtained upon crystallization from these mixtures (see below).

In the case of the rhenium compound **8**, decarbonylation does not take place spontaneously at room temperature, but it can be easily induced by heating toluene solutions of the complex at 343 K for ca. 2.5 h to give an analogous complex $[Mo_4Re_2Cp_4(\mu\text{-}PCy_2)_2(\mu_4\text{-}\kappa^1\text{:}\kappa^2\text{:}\kappa^2\text{:}\kappa^1\text{-}P_2)_2(CO)_{12}]$ (**10**), also obtained as a mixture of isomers **R** and **M** in similar amounts. The symmetrical isomer **10R**, however, was more air-sensitive than **10M**, leading to mixtures with higher proportions of the isomer **10M** after manipulation, which allowed the identification of most resonances of these isomers.

Solid-State Structure of Compounds 9 and 10. The structure of the isomer **9M** was determined through an X-ray diffraction analysis. Although the quality of the data was rather poor, it allowed us to determine the connectivity of the atoms and the relative disposition of the different groups (Figure 4 and Table 6). The molecule of **9M** is built from two similar substructures having a pseudotetrahedral Mo_2P_2 core bound to two $Mn(CO)_4$ fragments, defining a Mn_2P_4 six-membered ring in an unusual "boat" conformation. We note that related compounds with hexagonal M_2P_4 cores (M = Ag,[4b] Cu,[4b] Re,[24] Mo[25]) have been already described in the literature, but the conformation of these rings typically are either planar or "chair-like". The geometry around the Mn atoms is almost perfectly octahedral and deserves no comments. As for the Mo_2P_2 subunits, each of them has the same transoid geometry found

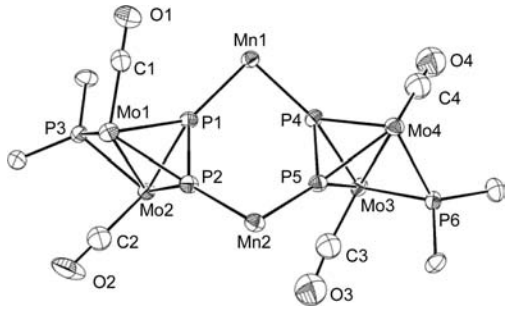

Figure 4. ORTEP diagrams (30% probability) of compound **9** (isomer **M**) with H atoms, Cy groups (except the C^1 atoms), Cp, and Mn-bound CO ligands omitted for clarity.

Table 6. Selected Bond Lengths (Å) and Angles (deg) for Isomer 9M

Mo1−Mo2	2.978(1)	Mo2−Mo1−C1	118.4(5)
Mo3−Mo4	3.002(1)	Mo1−Mo2−C2	78.5(4)
P1−P2	2.076(4)	Mo4−Mo3−C3	115.5(5)
P4−P5	2.074(4)	Mo3−Mo4−C4	82.0(5)
Mo1−P1	2.513(2)	P1−P2−Mn2	131.6(1)
Mo1−P2	2.481(3)	P2−P1−Mn1	131.0(1)
Mo1−P3	2.430(3)	P4−P5−Mn2	130.2(1)
Mo2−P1	2.476(2)	P5−P4−Mn1	132.4(1)
Mo2−P2	2.474(3)	P1−Mn1−P4	89.9(1)
Mo2−P3	2.432(2)	P2−Mn2−P5	90.5(1)
Mo1−C1	1.90(1)		
Mo2−C2	1.98(2)		
Mn1−P1	2.389(3)		
Mn2−P2	2.392(3)		

in the iron compound **4** but corresponds to a different optical isomer, so although the different ligands are pairwise related, they are not strictly equivalent. This applies, for instance, to the PCy_2 ligands (P3 and P6), carbonyls bent over the corresponding Mo−Mo bonds (C2 and C4, C−Mo−Mo ca. 80°), or carbonyls pointing away from it (C1 and C3, C−Mo−Mo ca. 120°). The most significant difference with the structure of **4** of course is the coordination of both P atoms of each diphosphorus ligand to Mn atoms (type **II** structure), with similar Mn−P lengths of ca. 2.39 Å. As a result, the P^{bs}−Mo and P^{ap}−Mo bonds become of comparable length (ca. 2.47 Å). Notably, the P−P length seems to be unaffected by the coordination of the μ-P_2 ligand to an additional metal atom and remains quite short (ca. 2.07 Å), as found in the type **I** derivatives of the anion **1** (cf. 2.089(2) Å in **4**).

Crystals of the rhenium compound **10** turned out to have both isomers **10M** and **10R** disordered in the unit cell with similar occupancy, and we could not obtain a fully anisotropic

dx.doi.org/10.1021/ic401204j | Inorg. Chem. 2013, 52, 9005−9018

model of the atomic positions, although the general geometrical features of the molecules were again well-defined. The structure of the isomer **10M** is analogous to that of **9M** and will not be discussed. The structure of the isomer **R** (Figure 5 and Table 7)

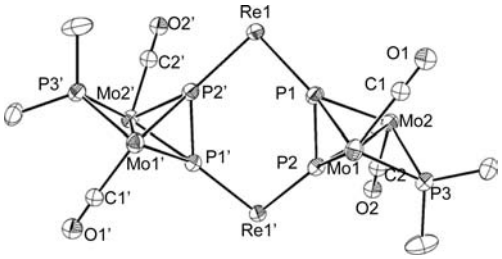

Figure 5. ORTEP diagrams (30% probability) of compound **10** (isomer **R**, 50% in the crystal), with H atoms, Cy groups (except the C^1 atoms), Cp, and Re-bound CO ligands omitted for clarity.

Table 7. Selected Bond Lengths (Å) and Angles (deg) for Isomer 10R

Mo1−Mo2	2.984(1)	Mo2−Mo1−C1	78.3(5)
P1−P2	2.072(3)	Mo1−Mo2−C2	115.2(5)
Mo1−P1	2.471(2)	P1−Re1−P2′	89.8(1)
Mo1−P2	2.478(3)	P2−P1−Re1	130.1(1)
Mo1−P3	2.430(3)	P1−P2−Re1′	132.3(1)
Mo2−P1	2.484(2)	C1−Mo1−P1	127.2(5)
Mo2−P2	2.490(3)	C1−Mo1−P2	86.9(5)
Mo2−P3	2.428(3)	C1−Mo1−P3	84.2(5)
Mo1−C1	2.03(2)	C2−Mo2−P1	71.1(5)
Mo2−C2	1.93(2)	C2−Mo2−P2	111.9(6)
Re1−P1	2.511(2)	C2−Mo2−P3	93.8(6)
Re1′−P2	2.512(2)		

is built from identical Mo_2P_2 subunits connected to two $Re(CO)_4$ moieties and defining a six-membered Re_2P_4 ring also with a "boat" conformation. As a result, there is a C_2 symmetry axis relating both Mo_2P_2 subunits and the Re fragments. Apart from this, we note that the interatomic distances and angles within each Mo_2P_2 subunit are comparable to those in **9M**, while the P−Re lengths are comparable to each other (ca. 2.51 Å), and the P−P length in the diphosphorus ligand remains quite short (2.072(3) Å).

Solution Structure of Compounds 9 and 10. The IR spectrum of the isomer **9M** in dichloromethane solution exhibits six bands in the range 2100−1950 cm^{-1}, the expected region for C−O stretches from $Mn(CO)_4$ fragments,[16] possibly indicating some vibrational coupling between the $Mn(CO)_4$ fragments of the molecule, which in any case are strictly inequivalent. In addition, the spectrum displays two additional and broader bands at 1888 and 1827 cm^{-1}, originated from the $Mo_2(CO)_2$ oscillators of the molecule. By comparing this spectrum with that of a mixture of isomers **M** and **R**, we could identify two bands of the isomer **9R** at 2061 (m) and 2001 (s) cm^{-1}, while the rest overlap with those of **9M**. As for the rhenium compound **10**, no individual assignment of the C−O stretches was possible because we could not separate both isomers. In any case, the observed bands were comparable to those of its manganese counterpart (Table 2).

The $^{31}P\{^1H\}$ NMR spectra of isomers **9M** and **9R** in CD_2Cl_2 solution at room temperature exhibit in each case a triplet (J_{PP} ca. 19 Hz) for the PCy_2 groups, while the P_2 ligands give rise to just one broad resonance at ca. −185 ppm, thus revealing a dynamic behavior comparable to those discussed for compounds **4**−**8**. In line with this, the ^1H NMR spectra at room temperature exhibit just one resonance for the four Cp ligands in each case. According to the solid-state structure of these isomers, six ^{31}P and four Cp resonances should be expected for the asymmetric isomer **9M**, these being reduced to three ^{31}P and two Cp resonances for the more symmetrical isomer **9R**. Unfortunately, no splitting was observed in the corresponding PCy_2 or ^1H NMR resonances of these isomers down to 190 K. As for the broad P_2 resonances, they further broadened upon cooling, and at ca. 218 K, they disappeared into the baseline of the spectrum but did not reappear still at 190 K. Thus, although the rate of exchange process involving the inequivalent P atoms of the diphosphorus ligands obviously had been reduced at low temperature, no useful information could be obtained from these data.

The rhenium compound **10** displayed a dynamic behavior comparable to that of **9**, although a bit slower, this in turn enabling us to identify in solution the inseparable isomers **M** and **R** (see the Experimental Section). At room temperature, the $^{31}P\{^1H\}$ NMR spectrum of each isomer displayed a triplet PCy_2 resonance at ca. 161 ppm (J_{PP} = 22 Hz), while the P_2 ligands gave rise to just a broad resonance at ca. −276.0 ppm. At the same time, the ^1H NMR spectrum displayed a single Cp resonance in each case. On lowering the temperature, a broadening in some of the resonances was observed and some splitting eventually occurred. At 178 K, the ^{31}P resonances of the major isomer had split into six broad signals, two PCy_2 resonances at 153.8 and 145.5 ppm and two sets of upfield broad doublets corresponding to two inequivalent P_2 units, with large one-bond couplings (δ−230.8 and −335.5 ppm, J_{PP} > 370 Hz, and δ −254.8 and −320.5 ppm, J_{PP} > 450 Hz) in agreement with the short P−P lengths of ca. 2.07 Å measured in the crystal. We can therefore assign all these resonances to the asymmetric isomer **10M**. Unfortunately, the resonances for the minor isomer could not be identified clearly in the low-temperature spectra, either because of their superimposition with those of the major isomer (PCy_2) or disappearance into the baseline of the spectrum (P_2), as observed for the manganese compound **9**.

To explain the above observations we must assume that for both compounds, the isomers **M** and **R** undergo a local exchange between the P^{ap} and P^{bs} positions within each Mo_2P_2 subunit not very different from that proposed for the trinuclear compounds **4**−**8** (Scheme 2). We note that in the case of the asymmetric isomers **M**, the above process also implies the effective equivalence between both Mo_2P_2 subunits, in agreement with the averaged spectrum observed at room temperature. From the coalescence temperatures of the PCy_2 (ca. 198 K) and Cp (ca. 183 K) resonances in the isomer **10M**, we can estimate an activation energy of 36 ± 1 kJ/mol for this

Scheme 2. Local Exchange Process Proposed for Compounds 9 and 10 in Solution

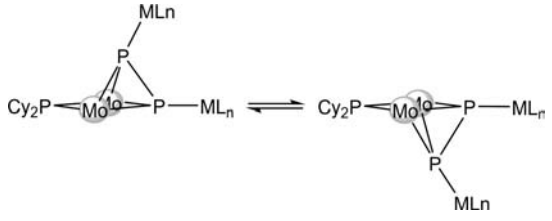

dx.doi.org/10.1021/ic401204j | Inorg. Chem. 2013, 52, 9005−9018

process, which is somewhat lower than the barrier measured for the trinuclear rhenium compound **8** (39 kJ/mol), likely because now all P atoms remain bound to the same metal fragments along the process.

CONCLUSION

The anionic diphosphorus complex **1** reacts with chlorophosphines to give unprecedented phosphinodiphosphenyl (P_2PR_2) complexes resulting from the insertion of the carbene-like PR_2^+ cations in one of the Mo−P^{bs} bonds of the anion. When R is the bulky ^{t}Bu group, this structure is slightly disfavored with respect to a type **I** structure (Chart 1) where the P^tBu_2 group is bound "end-on" to the basal P atom (computed P−P−P^tBu_2 angle 114.7°), thus avoiding unfavorable repulsions with the rest of the molecule. Presumably, structures analogous to the latter one are generated initially in the reactions with the less bulky chlorophosphines, which then rearrange rapidly via insertion in the basal Mo−P bond of the Mo_2P_2 tetrahedron. The reactions of the anion **1** with different transition-metal halide complexes [MXL_n] (with L being a Cp or CO ligand) lead in all cases to the "end-on" binding of the organometallic fragment ML_n to the basal P atom of the anion to give type **I** structures displaying P−P−M angles around 120°. Most of these complexes undergo a fluxional process involving the swing of the P_2 ligand around the Mo−Mo axis accompanied by the intramolecular exchange of the ML_n fragment between the P atoms of the diphosphorus ligand. This process is similar to the one previously observed for group 14 derivatives of **1** having structures of type **VI**, but slower, with Gibbs free energies of activation energy above ca. 40 kJ/mol, which is a sensible finding since structures of type **VI** might be found along the fluxional coordinate of the structures of type **I**, but not *vice versa*. Coordination of the apical P atom in these heterometallic derivatives could be forced through decarbonylation of the complexes having $M(CO)_5$ fragments (M = Mn, Re), this leading to dimeric structures having six-membered P_4M_2 rings in a "boat" conformation, with two $M(CO)_4$ fragments bridging two Mo_2P_2 tetrahedral units, which then display a local structure of type **II**. This brings about little structural changes within each Mo_2P_2 subunit, which still displays quite short P−P lengths of ca. 2.07 A, but facilitates the exchange between the inequivalent P sites of the diphosphorus ligand. All these heterometallic derivatives of **1** incorporate organometallic fragments having an odd number of electrons. However, from the reactions of **1** with chlorophosphines, it might be foreseen that carbene-like (i.e., 16-electron) organometallic fragments might react analogously with **1** to give related molecules displaying a novel coordination mode of the diphosphorus ligand (type **VIII** in Chart 1) and further work in that direction is being carried out currently in our laboratory.

EXPERIMENTAL SECTION

General Procedures and Starting Materials. All manipulations and reactions were carried out under a nitrogen (99.995%) atmosphere using standard Schlenk techniques. Solvents were purified according to literature procedures and distilled prior to use.[26] Compounds [$MnBr(CO)_5$],[27] [$ReCl(CO)_5$],[28] and [$FeClCp(CO)_2$],[29] as well as tetrahydrofuran solutions of Li[$Mo_2Cp_2(\mu\text{-}PCy_2)(\mu\text{-}\kappa^2\text{:}\kappa^2\text{-}P_2)(CO)_2$] (**1**),[7] were prepared as described previously, and all other reagents were obtained from the usual commercial suppliers and used as received, unless otherwise stated. Petroleum ether refers to that fraction distilling in the range 338−343 K. Chromatographic separations were carried out using jacketed columns refrigerated by tap water (ca. 288 K) or by a closed 2-propanol circuit kept at the desired temperature with a cryostat. Commercial aluminum oxide (activity I, 150 mesh) was degassed under vacuum prior to use. The latter was mixed afterward under nitrogen with the appropriate amount of water to reach the activity desired. IR stretching frequencies of CO ligands were measured in solution (using CaF_2 windows) and are referred to as ν(CO). Nuclear magnetic resonance (NMR) spectra were routinely recorded at 400.13 (^{1}H), 161.98 (^{31}P{^{1}H}), or 100.61 MHz (^{13}C{^{1}H}) at 295 K in CD_2Cl_2 solution unless otherwise stated. Chemical shifts (δ) are given in ppm, relative to internal tetramethylsilane (^{1}H, ^{13}C) or external 85% aqueous H_3PO_4 (^{31}P). Coupling constants (J) and line widths at half intensity of broad peaks ($\Delta\nu_{1/2}$) are given in hertz. P^{ap} and P^{bs} refer to the "apical" and "basal" P atoms of the Mo_2P_2 tetrahedron (see Chart 2).

*Preparation of [$Mo_2Cp_2(\mu\text{-}PCy_2)(\mu\text{-}\kappa^2_{P,P}\text{:}\kappa^2_{P,P''}\text{-}P_2PCy_2)(CO)_2$] (**2a**).* Neat PCy_2Cl (16 μL, 0.072 mmol) was added to a tetrahydrofuran solution (8 mL) containing ca. 0.050 mmol of **1**, and the mixture was stirred at room temperature for 15 min to give an orange-brownish solution. After removal of the solvent under vacuum, the residue was extracted with dichloromethane/petroleum ether (1:6), and the extracts were chromatographed through alumina. A yellow fraction was first eluted with the same solvent mixture, containing small amounts of [$Mo_2Cp_2(\mu\text{-}PCy_2)(\mu\text{-}PH_2)(CO)_2$], this being followed by an orange fraction which gave, after removal of solvents, compound **2a** as a yellow solid (0.028 g, 65%). The crystals used in the X-ray study were grown by the slow diffusion of a diethyl ether layer into a dichloromethane solution of the complex at 253 K. Anal. Calcd for $C_{36}H_{54}Mo_2O_2P_4$: C, 51.81; H, 6.52. Found: C, 51.66; H, 6.61. ^{1}H NMR (300.13 MHz): δ 5.28, 5.15 (2s, 2 × 5H, Cp), 2.60−1.20 (m, 44H, Cy). ^{31}P{^{1}H} NMR (121.50 MHz): δ 154.5 (s, μ-PCy_2), 74.8 (d, J_{PP} = 277, P^{ap}), −6.3 (dd, J_{PP} = 229, 277, P^{bs}), −19.6 (d, J_{PP} = 229, PCy_2).

*Preparation of [$Mo_2Cp_2(\mu\text{-}PCy_2)(\mu\text{-}\kappa^2_{P,P}\text{:}\kappa^2_{P,P''}\text{-}P_2PPh_2)(CO)_2$] (**2b**).* Neat PPh_2Cl (12 μL, 0.067 mmol) was added to a tetrahydrofuran solution (10 mL) containing ca. 0.060 mmol of **1**, and the mixture was stirred at room temperature for 15 min to give a yellow solution. Workup as described for **2a** (elution with dichloromethane/petroleum ether (1:8)) gave a yellow fraction containing small amounts of [$Mo_2Cp_2(\mu\text{-}PCy_2)(\mu\text{-}PH_2)(CO)_2$] and then an orange fraction yielding compound **2b** as a light orange solid (0.033 g, 67%). Anal. Calcd for $C_{36}H_{42}Mo_2O_2P_4$: C, 52.57; H, 5.15. Found: C, 52.66; H, 5.06. ^{1}H NMR (300.13 MHz): δ 7.78 (m, 2H, Ph), 7.50−7.40 (m, 5H, Ph), 7.35 (m, 2H, Ph), 7.27 (m, 1H, Ph), 4.99 (t, J_{HP} = 0.9, 5H, Cp), 4.90 (s, 5H, Cp), 2.3−1.1 (m, 22H, Cy). ^{31}P{^{1}H} NMR (121.50 MHz): δ 149.8 (s, μ-PCy_2), 71.9 (d, J_{PP} = 270, P^{ap}), 18.8 (dd, J_{PP} = 270, 252, P^{bs}), −25.0 (d, J_{PP} = 252, PPh_2). ^{13}C{^{1}H} NMR (C_6D_6): δ 245.6 (td, J_{CP} = 14, 3, MoCO), 244.2 (td, J_{CP} = 10, 2, MoCO), 146.0 (t, J_{CP} = 5, C^1−Ph), 136.2 (d, J_{CP} = 19, C^1−Ph), 132.6 (dd, J_{CP} = 10, 3, C^2−Ph), 131.0 (d, J_{CP} = 8, C^2−Ph), 129.6, 128.5 (2d, J_{CP} = 2, C^4−Ph), 128.4 (d, J_{CP} = 10, C^3−Ph), 128.3 (d, J_{CP} = 3, C^3−Ph), 90.1, 87.9 (2s, Cp), 50.8 (dd, J_{CP} = 6, 3, C^1−Cy), 46.5 (t, J_{CP} = 8, C^1−Cy), 37.2 (t, J_{CP} = 4, C^2−Cy), 35.6 (d, J_{CP} = 5, C^2−Cy), 35.5, 35.3 (2d, J_{CP} = 4, C^2−Cy), 29.1 (d, J_{CP} = 10, C^3−Cy), 29.1 (d, J_{CP} = 11, C^3−Cy), 28.7, 28.6 (2d, J_{CP} = 10, C^3−Cy), 26.9, 26.7 (2s, C^4−Cy).

*Reaction of **1** with ClP^tBu_2.* Neat P^tBu_2Cl (15 μL, 0.079 mmol) was added to a tetrahydrofuran solution (8 mL) containing ca. 0.050 mmol of **1**, and the mixture was then stirred at room temperature for 15 min to yield an orange-red solution. Workup as described for **2a** gave a yellow fraction containing small amounts of [$Mo_2Cp_2(\mu\text{-}PCy_2)(\mu\text{-}PH_2)(CO)_2$] and then a reddish fraction yielding a mixture of the isomers [$Mo_2Cp_2(\mu\text{-}PCy_2)(\mu\text{-}\kappa^2_{P,P'}\text{:}\kappa^2_{P,P''}\text{-}P_2P^tBu_2)(CO_2)$] (**2c**) and [$Mo_2Cp_2(\mu\text{-}PCy_2)(\mu\text{-}\kappa^2_{P,P'}\text{:}\kappa^2_{P,P''}\text{-}P_2P^tBu_2)(CO_2)$] (**3**) as a dark orange solid (0.025 g, 63%). In solution, these isomers are in equilibrium, with the ratio **3**/**2c** being ca. 7 at 295 K and 4:5 at 213 K, both in toluene-d_8 solution. Spectroscopic data for **2c**. ^{1}H NMR: δ 5.22, 5.17 (2s, 2 × 5H, Cp), 1.22 (d, J_{HP} = 11, 9H, ^{t}Bu). ^{1}H NMR (toluene-d_8, 295 K): δ 5.22, 4.97 (2s, 2 × 5H, Cp), 1.24 (s, 9H, ^{t}Bu); the resonance of the other ^{t}Bu group was masked by those of the major isomer **3**. ^{1}H NMR (toluene-d_8, 253 K, **2c**/**3** = 5:8): δ 5.19, 4.92 (2s, 2 × 5H, Cp), 2.1−1.0 (m, 22H, Cy), 1.09 (d, J_{HP} = 12, 9H, ^{t}Bu). ^{1}H NMR (toluene-d_8, 213 K, **2c**/**3** = 5:4): δ 5.17, 4.87 (2s, 2 × 5H, Cp), 2.1−1.0 (m, 22H,

dx.doi.org/10.1021/ic401204j | Inorg. Chem. 2013, 52, 9005−9018

Cy), 1.25 (d, J_{HP} = 10, 9H, ^{t}Bu), 1.06 (d, J_{HP} = 12, 9H, ^{t}Bu). $^{31}P\{^1H\}$ NMR: δ 144.6 (s, μ-PCy_2), 50.2 (d, J_{PP} = 286, P^{ap}), 18.2 (d, J_{PP} = 256, P^tBu_2), −23.6 (dd, J_{PP} = 286, 256, P^{bs}). $^{31}P\{^1H\}$ NMR (toluene-d_8, 295 K): δ 142.4 (s, μ-PCy_2), 52.4 (d, J_{PP} = 289, P^{ap}), 16.6 (d, J_{PP} = 258, P^tBu_2), −18.4 (dd, J_{PP} = 289, 259, P^{bs}). $^{31}P\{^1H\}$ NMR (toluene-d_8, 253 K): δ 142.1 (s, μ-PCy_2), 50.0 (d, J_{PP} = 293, P^{ap}), 18.6 (d, J_{PP} = 263, P^tBu_2), −21.5 (dd, J_{PP} = 293, 263, P^{bs}). Spectroscopic data for **3**. ^1H NMR: δ 5.21, 5.19 (2s, 2 × 5H, Cp), 2.2−1.1 (m, 22H, Cy), 1.35, 1.26 (2d, J_{HP} = 11, 2 × 9H, ^{t}Bu). ^1H NMR (toluene-d_8, 295 K): δ 5.14, 5.01 (2s, 2 × 5H, Cp), 1.9−1.0 (m, 22H, Cy), 1.30, 1.26 (2d, J_{HP} = 12, 2 × 9H, ^{t}Bu). ^1H NMR (toluene-d_8, 253 K): δ 5.14, 4.96 (2s, 2 × 5H, Cp), 2.20−1.40 (m, 22H, Cy), 1.28, 1.25 (2d, J_{HP} = 12, 2 × 9H, ^{t}Bu). ^1H NMR (toluene-d_8, 213 K): δ 5.14, 4.89 (2s, 2 × 5H, Cp), 2.04−1.40 (m, 22H, Cy), 1.28, 1.25 (2d, J_{HP} = 12, 2 × 9H, ^{t}Bu). $^{31}P\{^1H\}$ NMR: δ 149.2 (t, J_{PP} ca. 11, μ-PCy_2), 47.9 (d, J_{PP} = 446, P^tBu_2), −168.4 (td, J_{PP} = 446, 8, P^{bs}), −184.1 (dd, J_{PP} = 446, 14, P^{ap}). $^{31}P\{^1H\}$ NMR (toluene-d_8, 295 K): δ 147.8 (t, J_{PP} = 10, μ-PCy_2), 48.2 (d, J_{PP} = 450, P^tBu_2), −165.3 (td, J_{PP} = 450, 7, P^{bs}), −184.1 (dd, J_{PP} = 450, 11, P^{ap}). $^{31}P\{^1H\}$ NMR (toluene-d_8, 253 K): δ 147.8 (t, J_{PP} = 11, μ-PCy_2), 45.6 (d, J_{PP} = 450, P^tBu_2), −166.6 (td, J_{PP} = 450, 11, P^{bs}), −189.8 (d, J_{PP} = 450, P^{ap}).

*Preparation of [$Mo_2FeCp_3(\mu$-$PCy_2)(\mu_3$-κ^2:κ^2:κ^1-$P_2)(CO)_4$] (**4**).* Solid [$FeClCp(CO)_2$] (0.017 g, 0.079 mmol) was added to a tetrahydrofuran solution (14 mL) containing ca. 0.075 mmol of **1**, and the mixture was stirred at room temperature for 15 min to give a red solution. Workup as described for **2a** gave a yellow fraction containing small amounts of [$Mo_2Cp_2(\mu$-$PCy_2)(\mu$-$PH_2)(CO)_2$]. Then a dark pink fraction was eluted with dichloromethane/petroleum ether (1:2), which yielded, after removal of solvents, compound **4** as a dark pink solid (0.041 g, 67%). The crystals used in the X-ray study were grown by slow diffusion of a petroleum ether layer into a toluene solution of the complex at 278 K. Anal. Calcd for $C_{31}H_{37}FeMo_2O_4P_3$: C, 45.73; H, 4.58. Found: C, 45.60; H, 4.65. ^1H NMR: δ 5.18 (s, 10H, CpMo), 5.01 (s, 5H, CpFe), 2.0−1.1 (m, 22H, Cy). ^1H NMR (208 K): δ 5.20 (s, br, 10H, CpMo), 5.08 (s, 5H, CpFe), 2.0−1.1 (m, 22H, Cy). ^1H NMR (198 K): δ 5.20, 5.19 (2s, 2 × 5H, CpMo), 5.09 (s, 5H, CpFe), 2.0−1.1 (m, 22H, Cy). $^{31}P\{^1H\}$ NMR: δ 161.9 (t, J_{PP} = 13, PCy_2), −50 (vbr, PFe), −220 (vbr, P^{ap}). $^{31}P\{^1H\}$ NMR (278 K): δ 162.0 (t, J_{PP} = 13, PCy_2), −52.6 (br, PFe), −224.7 (br, P^{ap}). $^{31}P\{^1H\}$ NMR (238 K): δ 162.3 (t, J_{PP} = 13, PCy_2), −53.5 (d, J_{PP} = 491, PFe), −228.9 (d, J_{PP} = 491, P^{ap}). $^{31}P\{^1H\}$ NMR (178 K): δ 163 (br, PCy_2, isomers **4A** and **4B**), −46.5 (s, br, PFe, isomer **4B**), −58.6 (d, br, J_{PP} > 440, PFe, isomer **4A**), −234.7 (d, J_{PP} = 494, P^{ap}, isomers **4A** and **4B**). $^{13}C\{^1H\}$ NMR (75.47 MHz): δ 238.4 (dd, J_{CP} = 25, 8, MoCO), 212.5 (t, J_{CP} = 8, FeCO), 211.9 (t, J_{CP} = 10, FeCO), 86.8 (s, CpFe), 85.5 (s, CpMo), 46.7 (br, C^1−Cy), 34.2 (s, br, C^2−Cy), 34.0 (d, J_{CP} = 3, C^2−Cy), 27.8 (d, J_{CP} = 11, C^3−Cy), 27.3 (d, J_{CP} = 9, C^3−Cy), 25.7 (s, C^4−Cy). $^{13}C\{^1H\}$ NMR (198 K): δ 241.3 (d, J_{CP} = 35, MoCO), 238.4 (br, MoCO), 213.9 (d, J_{CP} = 16, FeCO), 213.1 (d, J_{CP} = 20, FeCO), 89.9 (s, CpMo), 86.8 (s, CpFe), 85.8 (s, CpMo), 51.2 (br, C^1−Cy), 51.1 (br, C^1−Cy), 35.9, 35.5, 34.2, 33.3 (4s, C^2−Cy), 28.8, 28.5 (2d, J_{CP} = 11, C^3−Cy), 28.2 (d, J_{CP} = 7, C^3−Cy), 28.0 (d, J_{CP} = 10, C^3−Cy), 26.7, 26.6 (2s, C^4−Cy).

*Preparation of [$Mo_3Cp_3(\mu$-$PCy_2)(\mu_3$-κ^2:κ^2:κ^1-$P_2)(CO)_5$] (**5**).* Solid [$MoCpI(CO)_3$] (0.016 g, 0.055 mmol) was added to a tetrahydrofuran solution (8 mL) containing ca. 0.050 mmol of **1** at 223 K, and the mixture was stirred while it was allowed to reach room temperature progressively for 1 h to give a brown solution. After removal of the solvent under vacuum, the residue was extracted with dichloromethane/petroleum ether (1:5), and the extracts were chromatographed through alumina at 253 K. A yellow fraction containing small amounts of [$Mo_2Cp_2(\mu$-$PCy_2)(\mu$-$PH_2)(CO)_2$] was first eluted using this solvent mixture. Elution with dichloromethane/petroleum ether (1:2) gave a maroon fraction yielding compound **5** as a maroon solid (0.030 g, 67%). Anal. Calcd for $C_{32}H_{37}Mo_3O_5P_3$: C, 43.56; H, 4.23. Found: C, 43.27; H, 4.40. ^1H NMR: δ 5.54 (s, 5H, Cp), 5.20 (s, 10H, Cp), 1.95−1.10 (m, 22H, Cy). ^1H NMR (245 K): δ 5.59 (s, 5H, Cp), 5.22 (s, br, 10H, Cp), 1.90−1.10 (m, 22H, Cy). ^1H NMR (208 K): δ 5.63 (s, 5H, Cp), 5.28, 5.17 (2s, 2 × 5H, Cp), 1.90−1.10 (m, 22H, Cy). $^{31}P\{^1H\}$ NMR: δ 157.9 (t, J_{PP} = 13, PCy_2). $^{31}P\{^1H\}$ NMR (270 K): δ 158.1 (t, J_{PP} = 13, PCy_2), −134.8 (br, PMo), −188.2 (br, P^{ap}). $^{31}P\{^1H\}$ NMR (258 K): δ 158.2 (t, J_{PP} = 13, PCy_2), −134.1 (d, br, J_{PP} = 480, PMo), −190.3 (d, br, J_{PP} = 480, P^{ap}). $^{31}P\{^1H\}$ NMR (240 K): δ 158.3 (t, J_{PP} = 13, PCy_2), −134.8 (d, J_{PP} = 480, PMo), −191.8 (d, J_{PP} = 480, P^{ap}).

*Preparation of [$Mo_2ZrClCp_4(\mu$-$PCy_2)(\mu_3$-κ^2:κ^2:κ^1-$P_2)(CO)_2$] (**6**).* Solid [$ZrCl_2Cp_2$] (0.016 g, 0.055 mmol) was added to a tetrahydrofuran solution (8 mL) containing ca. 0.050 mmol of **1**, and the mixture was then stirred at room temperature for 15 min to give a brown-yellowish solution. After removal of the solvent under vacuum, the remaining residue was extracted with petroleum ether (4 × 2.5 mL), and the extracts were filtered. Removal of the solvent from the yellow filtrate gave compound **6** as a yellow, quite air-sensitive solid (0.025 g, 55%). Thus, satisfactory elemental analysis of this product could not be obtained. ^1H NMR: δ 6.49, 6.30 (2s, 2 × 5H, ZrCp), 5.17, 5.02 (2s, 2 × 5H, MoCp), 2.45−1.10 (m, 22H, Cy). $^{31}P\{^1H\}$ NMR: δ 143.2 (s, μ-PCy_2), −129.7 (d, J_{PP} = 460, PZr), −320.3 (d, J_{PP} = 460, P^{ap}).

*Reaction of **1** with [$MnBr(CO)_5$].* Solid [$MnBr(CO)_5$] (0.019 g, 0.069 mmol) was added to a tetrahydrofuran solution (11 mL) containing ca. 0.070 mmol of **1** at 248 K, and the mixture was stirred at that temperature for 30 min to give a brown-yellowish solution, which was filtered. Removal of the solvent from the filtrate gave a brown solid containing [$Mo_2MnCp_2(\mu$-$PCy_2)(\mu_3$-κ^2:κ^2:κ^1-$P_2)(CO)_7$] (**7**) as the major species. Attempts to further purify this solid resulted in its progressive transformation into a mixture of isomers of compound **9** (see below). Spectroscopic data for **7**: ^1H NMR (300.13 MHz): δ 5.22 (s, J_{PH} = 1, 10H, Cp), 2.0−1.10 (m, 22H, Cy). $^{31}P\{^1H\}$ NMR (121.50 MHz): δ 155.6 (t, J_{PP} = 12, PCy_2), −168.4 (s, br, P_2).

*Preparation of [$Mo_2ReCp_2(\mu$-$PCy_2)(\mu_3$-κ^2:κ^2:κ^1-$P_2)(CO)_7$] (**8**).* Solid [$ReCl(CO)_5$] (0.028 g, 0.077 mmol) was added to a tetrahydrofuran solution (11 mL) containing ca. 0.070 mmol of **1**, and the mixture was stirred for 15 min to give a green-brownish solution. Workup as described for **2a** (elution with dichloromethane/petroleum ether (1:5)) gave a yellow fraction containing small amounts of [$Mo_2Cp_2(\mu$-$PCy_2)(\mu$-$PH_2)(CO)_2$] and then a brown fraction yielding compound **8** as a green-brownish solid (0.039 g, 59%). Anal. Calcd for $C_{29}H_{32}Mo_2O_7P_3Re$: C, 36.15; H, 3.35. Found: C, 35.90; H, 3.30. ^1H NMR: δ 5.17 (s, 10H, Cp), 2.0−1.1 (m, 22H, Cy). ^1H NMR (198 K): δ 5.20 (s, br, 10H, Cp), 2.0−1.1 (m, 22H, Cy). ^1H NMR (182 K): δ 5.21 (s, br, $\Delta\nu_{1/2} \approx 12$, 10H, Cp), 2.0−1.1 (m, 22H, Cy). ^1H NMR (178 K): δ 5.22 (s, br, $\Delta\nu_{1/2} \approx 8$, 5H, Cp), 5.20 (s, br, $\Delta\nu_{1/2} \approx 7$, 5H, Cp), 2.0−1.1 (m, 22H, Cy). ^1H NMR (173 K): δ 5.22, 5.20 (2s, 2 × 5H, Cp), 2.0−1.1 (m, 22H, Cy). $^{31}P\{^1H\}$ NMR: δ 154.4 (t, J_{PP} = 10, PCy_2), −220.7 (br, $\Delta\nu_{1/2} \approx 340$, P_2). $^{31}P\{^1H\}$ NMR (238 K): δ 154.4 (t, J_{PP} = 9, PCy_2), −203.4 (br, PRe), −255.3 (br, P^{ap}). $^{31}P\{^1H\}$ NMR (198 K): δ 154.8 (br, PCy_2), −200.8 (d, J_{PP} = 460, P^{ap}), −256.6 (d, br, J_{PP} > 440, PRe). $^{31}P\{^1H\}$ NMR (178 K): δ 155.0 (br, PCy_2), −203.4 (d, br J_{PP} > 440, P^{ap}), −256.6 (d, vbr, J_{PP} > 430 PRe). $^{13}C\{^1H\}$ NMR (75.46 MHz): δ 238.6 (td, J_{CP} = 12, 9, MoCO), 182.2 (br, ReCO), 87.5 (s, Cp), 47.6 (d, J_{CP} = 11, C^1−Cy), 35.3 (d, J_{CP} = 2, C^2−Cy), 35.3 (d, J_{CP} = 4, C^2−Cy), 28.9 (d, J_{CP} = 11, C^3−Cy), 28.5 (d, J_{CP} = 9, C^3−Cy), 26.9 (d, J_{CP} = 1, C^4−Cy). $^{13}C\{^1H\}$ NMR (183 K): δ 240.8 (d, br, J_{CP} = 34, MoCO), 237.8 (br, MoCO), 182.3 (s, br, ReCO), 177.1 (d, br, J_{CP} = 31, ReCO), 89.5, 85.3 (2s, Cp), 50.6 (d, J_{CP} = 10, C^1−Cy), 36.3, 35.1 (2s, br, C^2−Cy), 34.0 (s, br, $2C^2$−Cy), 28.6 (br, $2C^3$−Cy), 28.1 (br, $2C^3$−Cy), 26.6 (s, $2C^4$−Cy).

*Preparation of [$Mo_4Mn_2Cp_4(\mu$-$PCy_2)_2(\mu_4$-κ^1:κ^2:κ^2:κ^1-$P_2)_2(CO)_{12}$] (**9**).* The solvent was removed under vacuum from a crude tetrahydrofuran solution of **7** prepared from compound **1** (ca. 0.120 mmol) as described previously. The remaining residue was dissolved in dichloromethane/petroleum ether (1:5) and chromatographed through a short alumina column. Elution with the same mixture gave first a yellow fraction containing a small amount of [$Mo_2Cp_2(\mu$-$PCy_2)(\mu$-$PH_2)(CO_2)$] and then a brown fraction containing a mixture of compounds **7** and **9**. The solvents were then removed from this fraction, and the residue was dissolved in THF (5 mL) and stirred for 18 h at room temperature to give a mixture of isomers **9R** and **9M** in a 3:2 ratio. After removal of the solvent, this mixture was dissolved in dichloromethane/petroleum ether (1:6) and chromatographed

dx.doi.org/10.1021/ic401204j | Inorg. Chem. 2013, 52, 9005−9018

Table 8. Crystal Data for New Compounds

	2a	4·C_7H_8	9	10
mol formula	$C_{36}H_{54}Mo_2O_2P_4$	$C_{38}H_{45}FeMo_2O_4P_3$	$C_{56}H_{64}Mn_2Mo_4O_{12}P_6$	$C_{56}H_{64}Mo_4O_{12}P_6Re_2$
mol wt	834.55	906.38	1608.53	1871.07
cryst syst	monoclinic	monoclinic	monoclinic	monoclinic
space group	$P2_1/c$	$P2_1/c$	$P2_1/c$	$C2/c$
radiation (λ, Å)	1.54184	1.54184	1.54184	1.54184
a, Å	11.4768(2)	21.6108(3)	19.110(5)	22.0385(12)
b, Å	19.5895(3)	13.2744(2)	18.373(5)	18.5783(7)
c, Å	16.1293(2)	12.9822(2)	21.129(5)	19.1055(10)
α, deg	90	90	90	90
β, deg	98.1040(10)	98.3700(10)	114.284(5)	117.887(7)
γ, deg	90	90	90	90
V, Å^3	3590.05(9)	3684.54(9)	6762(3)	6914.1(6)
Z	4	4	4	4
calcd density, g cm^{-3}	1.544	1.634	1.58	1.794
absorp coeff, mm^{-1}	7.643	10.151	10.624	14.162
temp, K	100(2)	100(2)	150(2)	150(2)
θ range (deg)	3.57 to 68.55	3.92 to 74.56	3.32 to 75.05	3.29 to 74.43
index ranges (h, k, l)	−10, 13; −16, 23; −18, 19	−26, 24; −16, 11; −15, 14	−16, 23; −21, 22; −26, 21	−26, 27; −23, 21; −23, 16
reflns collected	16405	13402	25671	13405
indep reflns (R_{int})	6488 (0.0321)	7546 (0.0365)	13265(0.0589)	6820 (0.0610)
reflns with $I > 2\sigma(I)$	5486	6083	8083	5223
R indexes [data with $I > 2\sigma(I)$][a]	R_1 = 0.0279	R_1 = 0.0488	R_1 = 0.0941	R_1 = 0.0585
	wR_2 = 0.0653[b]	wR_2 = 0.1180[c]	wR_2 = 0.2679[d]	wR_2 = 0.1501[e]
R indexes (all data)[a]	R_1 = 0.0380	R_1 = 0.0582	R_1 = 0.1274	R_1 = 0.0748
	wR_2 = 0.0702[b]	wR_2 = 0.1221[c]	wR_2 = 0.3096[d]	wR_2 = 0.162[e]
GOF	1.051	1.107	1.09	1.055
no. of restraints/params	0/397	0/434	130/631	10/333
$\Delta\rho$ (max., min.), e Å^{-3}	0.811, −0.500	1.285, −1.635	3.656, −1.592	1.917, −2.161

[a] $R = \sum||F_o| - |F_c||/\sum|F_o|$. $wR = [\sum w(|F_o|^2 - |F_c|^2)^2 / \sum w|F_o|^2]^{1/2}$. $w = 1/[\sigma^2(F_o^2) + (aP)^2 + bP]$ where $P = (F_o^2 + 2F_c^2)/3$. [b] $a = 0.0334$, $b = 1.2558$. [c] $a = 0.0339$, $b = 17.6219$. [d] $a = 0.1795$, $b = 0.0000$. [e] $a = 0.0799$, $b = 4.3189$.

through alumina. Elution with the same solvent mixture gave a brown fraction yielding a mixture of the above isomers as a brown solid (0.098 g, 51% overall yield from **1**). The crystals of **9M** used in the X-ray study were grown by slow diffusion of a layer of petroleum ether into a dichloromethane solution of the mixture of isomers at 253 K. Anal. Calcd for $C_{56}H_{64}Mn_2Mo_4O_{12}P_6$ (**9M**): C, 41.81; H, 4.01. Found: C, 41.93; H, 3.73. Spectroscopic data for **9R**: ^{1}H NMR (300.13 MHz): δ 5.37 (s, 10H, Cp), 2.0−1.1 (m, 22H, Cy). ^{31}P{^{1}H} NMR (121.50 MHz): δ 165.2 (t, J_{PP} = 19, PCy_2), −184.0 (s, br, P_2). Spectroscopic data for **9M**: ^{1}H NMR (300.13 MHz): δ 5.39 (s, 10H, Cp), 2.0−1.10 (m, 22H, Cy). ^{31}P{^{1}H} NMR (121.50 MHz): δ 164.3 (t, J_{PP} = 21, PCy_2), −184.5 (s, br, P_2).

*Preparation of [$Mo_4Re_2Cp_4(\mu$-$PCy_2)_2(\mu_4$-κ^1:κ^2:κ^2:κ^1-$P_2)_2(CO)_{12}$] (**10**).* A solution of **8** (0.039 g, 0.040 mmol) in toluene (6 mL) was heated at 343 K for 1.5 h to give a brown solution containing a mixture of isomers **10R** and **10M** in similar amounts. After removal of the solvent, the residue was dissolved in dichloromethane/petroleum ether (1:5) and chromatographed through alumina. Elution with the same solvent mixture gave a brown fraction yielding a mixture of isomers **10R** and **10M** as a dark green solid (0.067 g, 89%). Crystals of **10** suitable for an X-ray analysis were grown by slow diffusion of a petroleum ether layer into a concentrated toluene solution of the mixture of isomers at 253 K. Both isomers were found to be present in the crystal lattice (see below). Anal. Calcd for $C_{56}H_{64}Mo_4O_{12}P_6Re_2$: C, 35.95; H, 3.45. Found: C, 35.67; H, 3.22. Spectroscopic data for **10R**: ^{1}H NMR: δ 5.33 (s, 20H, Cp), 2.0−1.1 (m, 44H, Cy). ^{1}H NMR (toluene-d_8): δ 5.235 (s, 20H, Cp), 2.0−1.2 (m, 44H, Cy); the resonances of **10R** in the ^{1}H NMR spectra were partly masked by those of the isomer **10M**. ^{31}P{^{1}H} NMR (121.50 MHz): δ 161.7 (t, J_{PP} = 23, PCy_2), −276.0 (s, br, P_2). ^{31}P{^{1}H} NMR (121.50 MHz, toluene-d_8): δ 160.9 (t, J_{PP} = 23, PCy_2), −276.7 (s, br, P_2). Spectroscopic data for **10M**: ^{1}H NMR: δ 5.31 (s, 20H, Cp), 2.0−1.1 (m, 44H, Cy). ^{1}H NMR (toluene-d_8, 295 K): δ 5.23 (s, 20H, Cp), 2.0−1.2 (m, 44H, Cy). ^{1}H NMR (toluene-d_8, 198 K): δ 5.16 (s, 20H, Cp), 2.0−1.1 (m, 44H, Cy). ^{1}H NMR (toluene-d_8, 178 K): δ 5.21, 5.11 (2s, br, 2 × 10H, Cp), 2.0−1.1 (m, 44H, Cy). ^{31}P{^{1}H} NMR (121.50 MHz): δ 160.9 (t, J_{PP} = 22, PCy_2), −276.0 (s, br, P_2). ^{31}P{^{1}H} NMR (toluene-d_8): δ 159.6 (t, J_{PP} = 23, PCy_2), −276.7 (s, br, P_2). ^{31}P{^{1}H} NMR (toluene-d_8, 198 K): δ 152.0 (br, J_{PP} = 23, PCy_2). ^{31}P{^{1}H} NMR (toluene-d_8, 178 K): δ 153.8 (s, br, PCy_2), 145.5 (s, br, PCy_2), −230.8 (d, br, J_{PP} > 370, P_2), −254.8 (d, br, J_{PP} > 450, P_2), −320.8 (d, br, J_{PP} > 450, P_2), −335.5 (d, br, J_{PP} > 370, P_2).

X-ray Structure Determination for Compounds 2a, 4, 9, and 10. Data collection for these compounds was performed on an Oxford Diffraction Xcalibur Nova single crystal diffractometer, using Cu Kα radiation (λ = 1.5418 Å) at 100 K (**2a** and 4·C_7H_8) or 150 K (**9** and **10**). Images were collected at a 100 mm (**2a**) or 63 mm fixed crystal-detector distance, using the oscillation method with 1° oscillation and variable exposure time per image (1.5−8 s for **2a**, 20−100 s for **4**, 10−20 s for **9**, and 9−30 s for **10**). Data collection strategy was calculated with the program CrysAlis Pro CCD (Oxford Diffraction Ltd., 2006).[29] Data reduction and cell refinement was performed with the program CrysAlis Pro RED (Oxford Diffraction Ltd., 2006).[30] An empirical absorption correction was applied using the SCALE3 ABSPACK algorithm as implemented in the program CrysAlis Pro RED (Oxford Diffraction Ltd., 2006).[30] Using the program suite WinGX,[31] the structures were solved by Patterson interpretation and phase expansion using SHELXL97[32] or SIR2 (**9**)[33] and refined with full-matrix least-squares on F^2 using SHELXL97. For all compounds, all non-hydrogen atoms were refined anisotropically, except those involved in disorder, and all hydrogen atoms were geometrically placed and refined using a riding model. Compound **4** crystallized with a

dx.doi.org/10.1021/ic401204j | Inorg. Chem. 2013, 52, 9005−9018

molecule of toluene. Compound **10** was found to be placed on a symmetry element (operation $x, y, 1/2 - z$), and carbonyl, Cp, and Cy groups were found to be disordered over two positions, corresponding to different isomers of the compound (**10R** and **10M**, see text). The best solution for the CO and Cp groups was obtained with occupancy factors of 0.55/0.45. The disorder in one of the cyclohexyl groups was satisfactorily modeled with occupancy factors of 0.6/0.40 on four of its carbon atoms. The other ring was modeled on five methylene carbon atoms with the above occupancy factors. Still, restraints in the C−C distances of one Cp ring had to be used to obtain a satisfactory model. During the refinement, a molecule of a nonidentified solvent was found to be present in the asymmetric unit; therefore, the SQUEEZE procedure,[34] as implemented in PLATON,[35] was used. Upon squeeze application and convergence, the strongest residual peak (1.92 eÅ^{-3}) was placed by the Mo(1) atom. For compound **9**, the Cp and Cy rings were somewhat disordered, but these could not be conveniently modeled due to poor quality of the diffraction data. Moreover not all the positional parameters and anisotropic temperature factors of non-H atoms could be refined anisotropically, and even some atoms had to be refined in combination with the instructions DELU and SIMU to achieve an anisotropic description. Thus an important number of atoms had to be refined isotropically to prevent their temperature factors from becoming nonpositive definite. Finally, some residual electron density corresponding to two molecules of nonidentified solvents were found to be present in the asymmetric unit; upon squeeze application and convergence, the strongest residual peak (2.15 e Å^{-3}) was placed close to a Cp ring. Crystallographic data and structure refinement details are collected in the Table 8.

Computational Details. All the DFT calculations were carried out using the GAUSSIAN03 package,[36] in which the hybrid method B3LYP was used with the Becke three-parameter exchange functional[37] and the Lee−Yang−Parr correlation functional.[38] An accurate numerical integration grid (99 590) was used for all the calculations via the keyword Int=Ultrafine. Effective core potentials and their associated double-ζ LANL2DZ basis set were used for the metal atoms.[39] The light elements (P, O, C, and H) were described with the 6-31G* basis.[40] Geometry optimizations were performed under no symmetry restrictions, using initial coordinates derived from the X-ray data of compounds **2a**, $[Mo_2Cp_2(\mu\text{-}PCy_2)(\mu\text{-}\kappa^2\text{:}\kappa^2\text{-}P_2Me)(CO)_2]$, and **4**. Frequency analyses were performed for all the stationary points to ensure that a minimum structure with no imaginary frequencies was achieved. Solvent effects (CH_2Cl_2) were modeled using the polarized-continuum-model of Tomasi and co-workers (PCM),[41] by using the gas-phase optimized structures. NMR shielding contributions and coupling constants were calculated using the gauge-including atomic orbitals (GIAO) method,[42] in combination with the LANL2DZ basis set for the Mo atoms and the IGLO-III basis set of Kutzelnigg and co-workers for the remaining atoms.[43]

■ ASSOCIATED CONTENT

Supporting Information

A CIF file containing full crystallographic data for compounds **2a**, **4**, **9**, and **10** and a file containing details of DFT calculations (drawings, selected geometric and NMR parameters, atomic coordinates and energies for compounds **2c**, **3**, and **4**). This material is available free of charge via the Internet at http://pubs.acs.org.

■ AUTHOR INFORMATION

Corresponding Author

*E-mail addresses: ara_12_79@hotmail.com (A.R.), mara@uniovi.es (M.A.R).

Notes

The authors declare no competing financial interest.

■ ACKNOWLEDGMENTS

We thank the DGI of Spain (Projects CTQ2009-09444 and CTQ2012-33187) and the European Commission (Project PERG08-GA-2010-276958) for financial support. A. R. thanks the Spanish Research Council for Scientific Research (CSIC) for a JAE-Doc contract, cofunded by the European Social Fund (ESF).

■ REFERENCES

(1) Vizi-Orosz, A.; Pályi, G.; Markó, L. *J. Organomet. Chem.* **1973**, *60*, C25.

(2) (a) Caporali, M.; Gonsalvi, L.; Rossin, A.; Peruzzini, M. *Chem. Rev.* **2010**, *110*, 4178. (b) Cossairt, B. M.; Piro, N. A.; Cummins, C. C. *Chem. Rev.* **2010**, *110*, 4164.

(3) See, for example: (a) Scherer, O. J.; Sitzmann, H.; Wolmerhauser, G. *J. Organomet. Chem.* **1986**, *309*, 77. (b) Scheer, M.; Schuster, K.; Krug, A.; Hartung, H. *Chem. Ber.* **1996**, *129*, 973. (c) Davies, J. E.; Mays, M. J.; Raithby, P. R.; Shields, G. P.; Tompkin, P. K.; Woods, A. D. *J. Chem. Soc., Dalton Trans.* **2000**, 1925.

(4) See, for example: (a) Bai, J.; Leiner, E.; Scheer, M. *Angew. Chem., Int. Ed.* **2002**, *41*, 783. (b) Scheer, M.; Gregoriades, L. J.; Zabel, M.; Bai, J.; Krossing, I.; Brunklaus, G.; Eckert, H. *Chem.—Eur. J.* **2008**, *14*, 282.

(5) (a) Abboud, J. L. M.; Herreros, M.; Notario, R.; Esseffar, M.; Mo, O.; Yañez, M. *J. Am. Chem. Soc.* **1996**, *118*, 1126. (b) Abboud, J. L. M.; Alkorta, I.; Dávalos, J. Z.; Gal, J. F.; Herreros, M.; Maria, P. C.; Notario, R.; Mo, O.; Molina, M. T.; Yañez, M. *J. Am. Chem. Soc.* **2000**, *122*, 4451.

(6) Welsch, S.; Lescop, C.; Balazs, G.; Réau, R.; Scheer, M. *Chem.—Eur. J.* **2011**, *17*, 9130.

(7) (a) Alvarez, M. A.; García, M. E.; García-Vivó, D.; Ramos, A.; Ruiz, M. A. *Inorg. Chem.* **2011**, *50*, 2064. (b) Alvarez, M. A.; García, M. E.; García-Vivó, D.; Ramos, A.; Ruiz, M. A. *Inorg. Chem.* **2012**, *51*, 11061.

(8) *In situ* formation and subsequent trapping of an anionic species obtained from the deprotonation of the neutral diphosphorus complex $[Mo_2Cp_2(CO)_3(\mu\text{-}\kappa^2\text{:}\kappa^2\text{-}P_2)(PHPh_2)]$ with DBU has been previously reported, although the negative charge is apparently located at the terminal PR_2 ligand according to the reactivity described for this anion. See: (a) Davies, J. E.; Mays, M. J.; Raithby, P. R.; Shields, G. P.; Tompkin, P. K. *Chem. Commun.* **1996**, 2051. (b) Davies, J. E.; Feeder, N.; Mays, M. J.; Tompkin, P. K.; Woods, A. D. *Organometallics* **2000**, *19*, 984.

(9) Selected spectroscopic data for $[Mo_2Cp_2(\mu\text{-}PCy_2)(\mu\text{-}PH_2)(CO)_2]$. ν(CO) (CH_2Cl_2): 1837 cm^{-1}. ^{1}H NMR (300.09 MHz, CD_2Cl_2, 298 K): δ 5.41 (s, 10H, Cp), 4.23 (dd, J_{PH} = 364, 2, 2H, PH_2), 2.4−1.1 (m, 22H, Cy) ppm. $^{31}P\{^1H\}$ NMR (121.48 MHz, CD_2Cl_2, 298 K): δ 116.3 (d, J_{PP} = 9, PCy_2), −74.3 (d, J_{PP} = 9, PH_2) ppm.

(10) García, M. E.; Riera, V.; Rueda, M. T.; Ruiz, M. A.; Sáez, D. *Organometallics* **2002**, *21*, 5515.

(11) Giffin, N. A.; Masuda, J. D. *Coord. Chem. Rev.* **2011**, *255*, 1342.

(12) (a) Krossing, I.; Raabe, I. *Angew. Chem., Int. Ed.* **2001**, *40*, 4406. (b) Weigand, J. J.; Holthausen, M.; Frohlich, R. *Angew. Chem., Int. Ed.* **2009**, *48*, 295.

(13) (a) Riera, V.; Ruiz, M. A.; Villafañe, F.; Bois, C.; Jeannin, Y. *Organometallics* **1993**, *12*, 124. (b) Alvarez, M. A.; García, M. E.; Ramos, A.; Ruiz, M. A. *Organometallics* **2007**, *26*, 1461. (c) Alvarez, M. A.; García, M. E.; Ramos, A.; Ruiz, M. A.; Lanfranchi, M.; Tiripicchio, A. *Organometallics* **2007**, *26*, 5454. (d) García, M. E.; García-Vivó, D.; Ruiz, M. A. *J. Organomet. Chem.* **2010**, *695*, 1592. (e) Alvarez, M. A.; García, M. E.; Menéndez, S.; Ruiz, M. A. *Organometallics* **2011**, *30*, 3694.

(14) (a) Grubba, R.; Wisniewska, A.; Baranowska, K.; Matern, E.; Pikies, J. *Polyhedron* **2011**, *30*, 1238. (b) Goesmann, H.; Matern, E.; Olkowska-Oetzel, J.; Pikies, J.; Fritz, G. *Z. Anorg. All. Chem.* **2001**, *627*, 1181.

(15) Caporalli, M.; Barbaro, P.; Gonsalvi, L.; Ienco, A.; Yakhvarov, D.; Peruzzini, M. *Angew. Chem., Int. Ed.* **2008**, *47*, 3766.

(16) Braterman, P. S. *Metal Carbonyl Spectra*; Academic Press: London, U. K., 1975.
(17) Harris, R. K.; Norval, E. M.; Fild, M. *J. Chem. Soc., Dalton Trans.* **1979**, 826.
(18) Jameson, C. J. in *Phosphorus-31 NMR Spectroscopy in Stereochemical Analysis*; Verkade, J. G., Quin, L. D., Eds.; VCH: Deerfield Beach, FL, 1987, Chapter 6.
(19) (a) Koch, W.; Holthausen, M. C. *A Chemist's Guide to Density Functional Theory*, 2nd ed.; Wiley-VCH: Weinheim, Germany, 2002. (b) Ziegler, T. *Chem. Rev.* **1991**, *91*, 651. (c) Foresman, J. B.; Frisch, Æ. *Exploring Chemistry with Electronic Structure Methods*, 2nd ed.; Gaussian, Inc.: Pittsburg, PA, 1996.
(20) Cramer, C. J. *Essentials of Computational Chemistry*, 2nd ed.; Wiley: Chichester, U. K., 2004.
(21) (a) Mirabello, V.; Caporali, M.; Gallo, V.; Gonsalvi, L.; Ienco, A.; Latronico, M.; Mastrorilli, P.; Peruzzini, M. *Dalton Trans.* **2011**, *40*, 9668. (b) Mirabello, V.; Caporali, M.; Gallo, V.; Gonsalvi, L.; Gudat, D.; Frey, W.; Ienco, A.; Latronico, M.; Mastrorilli, P.; Peruzzini, M. *Chem.—Eur. J.* **2012**, *18*, 11238.
(22) According to the modified Eyring equation $\Delta G^{\ddagger}_{Tc} = 19.14T_c[9.97 + \log(T_c/\Delta_\nu)]$ (J/mol). See: Günter, H. *NMR Spectroscopy*; John Wiley: Chichester, U.K., 1980; p 243.
(23) Wrackmeyer, B.; Alt, H. G.; Maisel, H. E. *J. Organomet. Chem.* **1990**, *399*, 125.
(24) Scherer, O. J.; Sitzmann, H.; Wolmershäuser, G. *J. Organomet. Chem.* **1984**, *23*, 968.
(25) Umbarkar, S.; Sekar, P.; Scheer, M. *J. Chem. Soc., Dalton Trans.* **2000**, 1135.
(26) Armarego, W. L. F.; Chai, C. *Purification of Laboratory Chemicals*, 5th ed.; Butterworth-Heinemann: Oxford, U. K., 2003.
(27) Quick, M. H.; Angelici, R. J. *Inorg Synth.* **1990**, *28*, 154.
(28) Schmidt, S. P.; Trogler, W. C.; Basolo, F. *Inorg. Synth.* **1990**, *28*, 160.
(29) Johnson, E. C.; Meyer, T. J.; Winterton, N. *Inorg. Chem.* **1971**, *10*, 218.
(30) *CrysAlis Pro*; Oxford Diffraction Ltd.: Oxford, U. K., 2006.
(31) Farrugia, L. J. *J. Appl. Crystallogr.* **1999**, *32*, 837.
(32) Sheldrick, G. M. *Acta Crystallogr.* **2008**, *A64*, 112.
(33) Altomare, A.; Cascarano, G.; Giacovazzo, C.; Guagliardi, A.; Burla, M. C.; Polidori, G.; Camalli, M. *J. Appl. Crystallogr.* **1994**, *27*, 435.
(34) Van der Sluis, P.; Spek, A. L. *Acta Crystallogr.* **1990**, *A46*, 194.
(35) Spek, A. L. *PLATON, A Multipurpose Crystallographic Tool*; Utrecht University: Utrecht, The Netherlands, 2010.
(36) Frisch, M. J.; Trucks, G. W.; Schlegel, H. B.; Scuseria, G. E.; Robb, M. A.; Cheeseman, J. R.; Montgomery, J. A., Jr.; Vreven, T.; Kudin, K. N.; Burant, J. C.; Millam, J. M.; Iyengar, S. S.; Tomasi, J.; Barone, V.; Mennucci, B.; Cossi, M.; Scalmani, G.; Rega, N.; Petersson, G. A.; Nakatsuji, H.; Hada, M.; Ehara, M.; Toyota, K.; Fukuda, R.; Hasegawa, J.; Ishida, M.; Nakajima, T.; Honda, Y.; Kitao, O.; Nakai, H.; Klene, M.; Li, X.; Knox, J. E.; Hratchian, H. P.; Cross, J. B.; Bakken, V.; Adamo, C.; Jaramillo, J.; Gomperts, R.; Stratmann, R. E.; Yazyev, O.; Austin, A. J.; Cammi, R.; Pomelli, C.; Ochterski, J. W.; Ayala, P. Y.; Morokuma, K.; Voth, G. A.; Salvador, P.; Dannenberg, J. J.; Zakrzewski, V. G.; Dapprich, S.; Daniels, A. D.; Strain, M. C.; Farkas, O.; Malick, D. K.; Rabuck, A. D.; Raghavachari, K.; Foresman, J. B.; Ortiz, J. V.; Cui, Q.; Baboul, A. G.; Clifford, S.; Cioslowski, J.; Stefanov, B. B.; Liu, G.; Liashenko, A.; Piskorz, P.; Komaromi, I.; Martin, R. L.; Fox, D. J.; Keith, T.; Al-Laham, M. A.; Peng, C. Y.; Nanayakkara, A.; Challacombe, M.; Gill, P. M. W.; Johnson, B.; Chen, W.; Wong, M. W.; Gonzalez, C.; Pople, J. A. *Gaussian 03*, revision B.02; Gaussian, Inc.: Wallingford, CT, 2003.
(37) Becke, A. D. *J. Chem. Phys.* **1993**, *98*, 5648.
(38) Lee, C.; Yang, W.; Parr, R. G. *Phys. Rev. B* **1988**, *37*, 785.
(39) Hay, P. J.; Wadt, W. R. *J. Chem. Phys.* **1985**, *82*, 299.
(40) (a) Hariharan, P. C.; Pople, J. A. *Theor. Chim. Acta* **1973**, *28*, 213. (b) Petersson, G. A.; Al-Laham, M. A. *J. Chem. Phys.* **1991**, *94*, 6081. (c) Petersson, G. A.; Bennett, A.; Tensfeldt, T. G.; Al-Laham, M. A.; Shirley, W. A.; Mantzaris, J. *J. Chem. Phys.* **1988**, *89*, 2193.
(41) (a) Cossi, M.; Barone, V.; Cammi, R.; Tomasi. *J. Chem. Phys. Lett.* **1996**, *255*, 327. (b) Fortunelli, A.; Tomasi. *J. Chem. Phys. Lett.* **1994**, *231*, 34. (c) Tomasi, J.; Persico, M. *Chem. Rev.* **1994**, *94*, 2027. (d) Floris, F.; Tomasi, J. *J. Comput. Chem.* **1989**, *10*, 616. (e) Pascual-Ahuir, J. L.; Silla, E.; Tomasi, J.; Bonaccorsi, R. J. *J. Comput. Chem.* **1987**, *8*, 778. (f) Mieritus, S.; Tomasi, J. *J. Chem. Phys.* **1982**, *65*, 239. (g) Mieritus, S.; Scrocco, E.; Tomasi, J. *J. Chem. Phys.* **1981**, *55*, 117.
(42) Wolinski, K.; Hinton, J. F.; Pulay, P. *J. Am. Chem. Soc.* **1990**, *112*, 8251.
(43) Kutzelnigg, W.; Fleischer, U.; Schindler, M. *NMR, Basic Princ. Prog.* **1990**, *23*, 165.